

International  
Progress Report

**IPR-01-54**

# Äspö Hard Rock Laboratory

**TRUE Block Scale project**

**Tracer test stage**

**Strategy for predictive modelling of  
transport of sorbing tracers in a  
fracture network**

Anders Winberg

Conterra AB

December 1999

**Svensk Kärnbränslehantering AB**

Swedish Nuclear Fuel  
and Waste Management Co  
Box 5864  
SE-102 40 Stockholm Sweden  
Tel +46 8 459 84 00  
Fax +46 8 661 57 19



**Äspö Hard Rock  
Laboratory**



Report no.  
IPR-01-54

Author  
Winberg

Checked by

Approved  
Christer Svemar

No.  
F56K

Date

Date

Date  
02-08-23

# **Äspö Hard Rock Laboratory**

## **TRUE Block Scale project**

### **Tracer test stage**

### **Strategy for predictive modelling of transport of sorbing tracers in a fracture network**

Anders Winberg

Conterra AB

December 1999

*Keywords:* Block scale, mass transfer, numerical model, prediction, sorbing, tracer

This report concerns a study which was conducted for SKB. The conclusions and viewpoints presented in the report are those of the author(s) and do not necessarily coincide with those of the client.



# Foreword

The following document constitutes the result of discussions on prediction strategy for tests with sorbing tracers planned as part of Phase C of the TRUE Block Scale Tracer Test Stage. During a modelling workshop in Bålsta, Sweden, Aug 30 through September 1, the contents and disposition of the report was drafted. The document has been compiled by the editor based on contributions from the various modelling team members. Contributions to the report have been obtained from:

Harrie-Jan Hendricks-Franssen, UPV (ENRESA)

Agustin Medina, UPC (ENRESA)

David Holton, AEAT (UK NIREX)

Bill Dershowitz, Golder Associates (JNC)

Antti Poteri, VTT Energy (POSIVA)

Review comments on earlier versions of this document have been extended by Peter Meier (ANDRA) and Peter Andersson (GEOSIGMA).

It should be noted that the detailed description and mathematical representation of the proposed approaches contained in the appendices of this report of necessity include some repetition and overlap in terms of basic common physics. The editor has intentionally retained these repetitions and overlaps.



# Abstract

The following document presents the approaches planned to be employed in the predictions of tests with sorbing tracers as part of Phase C of the TRUE Block Scale Tracer Test Stage. Premises of the planned work are presented in terms of objectives and general work scope. Further a tentative prediction case is presented. The proposed approaches include; the stochastic continuum (SC), the discrete fracture network (DFN), channel network (NC), the LaSAR and POSIVA approaches. The specific objectives and hypotheses are stated and the procedures of analyses are presented in an overview fashion as well as in a detailed mathematical context. In addition the common assumptions pertaining to conductive geometry, calibration data set, boundary conditions and common uncertainties are presented and discussed.





# Sammanfattning

Detta dokument presenterar de metoder som planeras att använda i prediktioner av tester med sorberande spårämnen som del i Fas C av TRUE Block Scale Tracer Test Stage. Förutsättningarna för det planerade arbetet presenteras i termer av syfte och generell arbetsomfattning. Vidare presenteras ett preliminärt prediktionsfall. De föreslagna metoderna inkluderar; stokastiskt kontinuum (SC), diskret spricknätverk (DNF), kanalnätverk (NC), LaSAR and POSIVA modellerna. De specifika syftena och hypoteserna är fastställda och analysprocedurer presenteras på en översiktlig sätt såväl som i ett detaljerat matematiskt sammanhang. Dessutom är de allmänna antagandena gällande konduktiv geometri, randvillkor och vanliga osäkerheter presenterade och diskuterade.



# Contents

<b>1</b>	<b>Introduction</b>	<b>1</b>
<b>2</b>	<b>Objectives and general work scope</b>	<b>3</b>
2.1	General	3
2.2	Objectives	3
2.3	Work scope	4
<b>3</b>	<b>Prediction case/-s</b>	<b>7</b>
3.1	General	7
3.2	Premises and principle layout of prediction case/-s	8
<b>4</b>	<b>Predictive approaches</b>	<b>9</b>
4.1	Stochastic continuum	9
4.1.1	Objectives	9
4.1.2	Basic assumptions and concepts	9
4.1.3	Implementation of the conceptual models	10
4.1.4	Calibration to prior data	12
4.1.5	Hypotheses testing	13
4.2	Discrete feature network	13
4.2.1	Objectives	13
4.2.2	Basic assumptions	14
4.2.3	Implementation	17
4.2.4	Uncertainty	18
4.2.5	Calibration	18
4.2.6	Hypothesis testing	18
4.3	Channel network approach	18
4.3.1	Objectives	18
4.3.2	Background	19
4.3.3	Model implementation	19
4.3.4	Calibration approach	21
4.3.5	Prediction approach	21
4.3.6	Evaluation approach	22
4.3.7	Approach to conceptual and parametric uncertainty	23
4.4	SKB/KTH-WRE LaSAR approach	23
4.4.1	Objectives	23
4.4.2	Basic concepts	23
4.4.3	Basic assumptions	24
4.4.4	Key parameters and prediction procedure	24

4.5	POSIVA/VTT approach	25
4.5.1	Objectives	25
4.5.2	Overview of approach	26
4.5.3	Basic assumptions and concepts	26
4.5.4	Prediction approach	27
<b>5.</b>	<b>Common assumptions</b>	<b>29</b>
5.1	Conductive geometry	29
5.2	Calibration data set	29
5.2.1	Material properties	29
5.2.2	Drawdown data	31
5.2.3	Tracer dilution data	31
5.2.4	Tracer breakthrough data	31
5.3	Boundary conditions	32
5.4	Common uncertainties	32
5.4.1	Conceptual uncertainty	32
5.4.2	Parametric uncertainty	33
<b>6.</b>	<b>Concluding remarks</b>	<b>35</b>
<b>7.</b>	<b>References</b>	<b>37</b>
	<b>Appendices</b>	<b>51</b>
A2.1	Introduction	55
A2.2	The Discrete Fracture Network Approach	56
A2.3	NAPSAC calculations	58
A2.4	Tracer transport	59
A2.5	The Rock-Matrix Diffusion and Sorption Model	60
A2.6	The Transport Algorithm	62
A2.7	Diffusion coefficients	64
A3.1	Flow modeling in FracMan/PAWorks	69
A3.1.1	Basic assumptions	69
A3.1.2	Geometric concepts	70
A3.1.3	Input parameters	70
A3.1.4	Spatial model	71
A3.1.5	Model scale	71
A3.1.6	Discretization	71
A3.1.7	Numerical solution	71

A3.2	PAWorks Transport models	72
A3.2.1	Basic assumptions	72
A3.2.2	Conceptual model	72
A3.2.3	Immobile zone	74
A3.2.4	Integration of flow and transport	74
A3.2.5	Input parameters	74
A3.2.6	Calibrated parameters	75
A3.2.7	Predicted entities and parameters	75
A3.2.8	Analytical/numerical solution	75
A3.3	References	77
A4.1	Flow modeling in LaSAR approach	81
A4.1.1	Basic assumptions	81
A4.1.2	Geometric concepts	81
A4.1.3	Input parameters	83
A4.1.4	Spatial model	83
A4.1.5	Model scale	83
A4.1.6	Discretization	83
A4.1.7	Numerical solution	83
A4.2	LaSAR Transport models	84
A4.2.1	Basic assumptions	84
A4.2.2	Conceptual model	85
A4.2.3	Immobile zone	86
A4.2.4	Integration of flow and transport	86
A4.2.5	Input parameters	86
A4.2.6	Calibrated parameters	87
A4.2.7	Predicted entities and parameters	87
A4.2.8	Analytical and numerical solution	87
A4.3	References	89
A5.1	POSIVA Transport model	93
A5.2	POSIVA supporting DFN flow modelling	94
A5.3	References	94

## List of Figures

Figure 4-1 Example of typical embedded 2D fracture and the associated 3D meshed planned to be used for transport calculations.

Figure 4-2 A schematic representation of a variable aperture fracture. The regions of enhanced porosity in the fracture control the water travel time. The narrow channels control the overall conductivity of the fracture. The transmissivity estimates provided by the hydraulic tests average over many flow channels and hence determine an averaged 'effective' aperture.

Figure 5-1 Reconciled March '99 Structural model including the trace of the new borehole KI0025F03. The shown deterministic structures with their interpreted extents are : Red = Structure #20, Light green = Structure #13, Violet = Feature #21, Dark Blue = Feature #22, Yellow = Structure #6, Light blue = Structure #19, Dark green = Structure #7, Pink = Structure #10.

## List of Tables

Table 1-1	ENRESA - Breakdown of flow model used in predictive modelling	41
Table 1-2	AEAT - Breakdown of flow model used in predictive modelling	42
Table 1-3	JNC/Golder - Breakdown of flow model used in predictive modelling	43
Table 1-4	SKB/LaSAR -Breakdown of flow model used in predictive modelling	44
Table 1-5	POSIVA - Breakdown of flow model used in predictive modelling	45
Table 2-1	ENRESA - Breakdown of transport model used in predictive modelling	46
Table 2-2	NIREX/AEAT - Breakdown of transport model used in predictive modelling	47
Table 2-3	JNC/Golder - Breakdown of transport model used in predictive modelling	48
Table 2-4	SKB/LaSAR - Breakdown of transport model used in predictive modelling	49
Table 2-5	POSIVA - Breakdown of transport model used in predictive modelling	50

# 1 Introduction

The TRUE Block Scale project is an international partnership funded by ANDRA, ENRESA, Nirex, POSIVA, JNC and SKB (Winberg, 1997). The Block Scale project is one part of the Tracer Retention Understanding Experiments (TRUE) conducted at the Äspö Hard Rock Laboratory. Presently the third of the defined stages, the Detailed Characterisation Stage, is coming to its conclusion. As a final step in the detailed characterisation a series of Pre-tests have been conducted with the aim of demonstrating the feasibility of performing tracer tests in the block scale.

The present stage, the Tracer Test Stage constitutes the final part in the experimental work, where the results of the performed characterisation and developed structural and hydraulic models are used as a basis for performing of a series of tracer tests on the block scale (L=10-50 m), including tests with sorbing tracers.

A programme has been presented (Winberg, in press) which provides the premises for the planned tests in terms of defined hypotheses, visualisations of the target experimental volume, results of pre-tests and hydraulic reconciliation of the most recent structural model. In addition, results of numerical design calculations and predictions of the tracer test performed as part of the Pre-tests are presented. Finally, an outline of the planned tracer tests programme for the Tracer Test Stage is presented.

In conjunction with the 9<sup>th</sup> Steering Committee Meeting July 1<sup>th</sup> it was identified that there is a need for the project group to present a unified strategy for the upcoming predictive modelling of the tests with sorbing tracers. The planned tests provide opportunity to test the predictive capability of transport models for a situation where, on the one hand, there is access to a wealth of structural and hydraulic information, supported by a limited data base of conservative tracer test results and tracer dilution data, and one on the other hand, there is access to no, or limited site-specific retention data.

An analogue to the above situation may prevail in a site selection situation, where two equitable sites have been investigated from the surface and there is a need to decide which of the two, from the standpoint of overall safety and performance, should be selected for detailed site characterisation, including access to the underground using a mined access route. For this assessment the analysts would have to rely on the existing data bases, including possible laboratory retention results (assumed limited), possible established links between site-characterisation data and relevant retention parameters (eg. link between resistivity of the rock (obtained from geophysical logs) and diffusivity), and retention data imported from relevant geological environments elsewhere.

The TRUE Block Scale project is in the situation that there exists relatively satisfactory structural and hydraulic models supported by tracer dilution data and a minor set of tracer breakthrough data. In order to inform our models for the purpose of predicting transport of sorbing tracers in a network, we have to rely on results from laboratory and field experiments conducted as part of TRUE-1, the latter implying tracer test results performed in a single fracture in the detailed scale (5-10 m) (Winberg, et al., 2000).

The Steering Committee has requested that a document detailing the project's plans for predictive modelling should be produced, and that this document should be subject to peer review as part of the 3<sup>rd</sup> TRUE Block Scale Review Meeting.

The present document provides :

- A definition of objectives and general work scope of the planned predictive modelling
- Premises and ramification for a foreseen prediction case for sorbing tracer transport
- An overview of the predictive approaches put forward, their specific objectives, the utilised concepts for flow and transport, their implementation and calibration to prior data.
- Assumptions common to all concepts/approaches



## **2 Objectives and general work scope**

### **2.1 General**

In the Tracer Test Programme (Winberg, in press), the important issues related to transport in a fracture network are identified. These issues are subsequently expressed in the form of hypotheses related to; conductive geometry, heterogeneity and retention. The objectives of the Tracer Test Stage have been presented by Winberg (in press):

- 1) To assess and quantify the parameters which control radionuclide retention in a fracture network in the block scale
- 2) To assess the predictive capability of developed block scale transport models and characterisation tools for predicting transport of sorbing tracers, and to evaluate which model assumptions are most appropriate and important.

Although the conductive geometry and heterogeneity are paramount entities which need to be satisfactory sorted out to resolve the effects of retention, the present document emphasises the retention aspects.

### **2.2 Objectives**

The principal objectives of the predictive modelling effort in relation to the planned tracer experiments with sorbing tracers are to;

- Demonstrate the level of understanding of transport of sorbing tracers in a fracture network in the block scale,
- Provide basis for identifying similarities and differences between the employed prediction approaches in the way they make use of input data, mode of calibration and predictive entities and parameters.

The key challenges related to the performance of the planned tracer tests and the associated modelling work are:

- can we perform an experiment(-s) that accounts for all non-flow and transport artefacts?
- can we parameterise the models sufficiently accurately, or account for the key uncertainties, with the data we can collect?
- is our understanding of flow and transport sufficiently complete to predict sorbing tracer tests?

Therefore, the overall modelling challenge consists of: can we provide a sufficiently 'realistic' model of flow and transport at a sufficiently detailed level that is possible to parameterise, by relatively unambiguous field data?

## 2.3 Work scope

The general work scope of the predictive task is to apply selected predictive approaches for the prediction of sorbing tracer transport, and in doing so making use of the available site-specific hydraulic data and conservative tracer test results, in combination with available tracer retention data from the laboratory (Byegård et al., 1998) and the detailed scale *in-situ* experiments carried out as part of TRUE-1 (Winberg, et al., 2000).

Representatives of the predictive approaches have been requested to specify their specific objectives and work scope within the overall framework mentioned above. This to allow the specific features of the employed models to be highlighted in the performed work.

It is identified that there is need to specify clearly what the basic concepts and assumptions, in relation to flow and transport, that are made by each approach. In this context, it is important to show how geometry and heterogeneity is treated/introduced, and how the transport processes are conceptualised, geometrically represented and parameterised. The latter includes clear identification of input parameters, which parameters that are calibrated to existing experimental results, and which prior retention data that are imported from elsewhere (eg. TRUE-1), and which specific parameters/entities of sorbing tracer transport that are actually being predicted.

The principal objective is addressed by employing predictive approaches which primarily has their origin in the modelling concepts for groundwater flow which have been used so far in the project, namely Stochastic Continuum (SC), Discrete Fracture Network (DFN), and Channel Network (CN). It is foreseen that these concepts, whether standalone or in combination, in the future will constitute tools which will be used in the assessment and screening of sites in a site selection process.

In addition, the semi-analytical Lagrangian Stochastic Advection-Reaction framework (LaSAR) (Cvetkovic et al., 1999), previously employed in the SKB TRUE team analysis of the TRUE-1 results (Winberg et al., 2000, Cvetkovic, et al, in prep), will be employed. The LASR approach can in practice be employed in a PA context. Hence, this approach, and its extension to a multiple fracture situation is a test of a tool which can be employed either in a (detailed) site screening situation, or in a PA evaluation of a selected site.

Finally, an approach is put forward by POSIVA, which for predictive purposes only make use of tracer dilution measurements supported by DFN modelling. This approach is featuring the importance to know the distribution of flow to make the necessary predictions. In this sense, it is of particular interest to the TRUE Block Scale partnership organisations since it only requires tracer dilution data, and no tracer experiments (breakthrough curves).



## **3 Prediction case/-s**

### **3.1 General**

The tracer test programme presented by Winberg (in press) outlines a staged approach made up of three different phases. The first of these, Phase A, emphasises testing of alternative sink sections, complementary tracer dilution tests, primarily in relation to potential new sink sections in the new borehole KI0025F03, followed by a tracer test using the identified optimal sink section. The latter test/-s is assumed to be similar to the tracer test (PT-4) performed as part of the Pre-tests (Andersson, et al., 1999) and will be subject to blind model predictions.

The following aspects of transport in a fracture network can potentially be addressed within the context of the Phase A tests;

- Anisotropy/heterogeneity within Structure #20
- Identification of suitable flow paths for sorbing tracer tests
- Reversal of flow fields
- Intersection effects

The subsequent phases, Phase B and C, are assumed to essentially constitute one long pumping in the selected sink. The initial part (Phase B) will include;

- Test of He-3 as a tracer in a fracture network context
- Demonstration of high recovery flow paths

The subsequent Phase C is focused on the tests with radioactive sorbing tracers, possibly including He-3 if demonstrated feasible. Phase B will not be subject to predictive work, only Phase C.

- Retention (weakly sorbing radioactive tracers)
- Indication of matrix diffusion effects using of He-3 as a tracer

It should be made clear that the project by no means at this time can clearly identify the exact flow path, or flow paths, in terms of selected sink section and candidate source (injection) sections, in which the tests with sorbing tracers will be run. However, below the selection of such set ups is discussed from a principal standpoint.

## 3.2 Premises and principle layout of prediction case/-s

It is assumed that the following assumptions and postulations apply to the conditions of performing the Phase C tests with sorbing tracers in the block scale;

- the primary goal is to collect tracer retention data from a flow path/-s which is known to involve multiple (>1) conductive structures.
- The shortest distance between sink and source is not considered as a critical parameter, as long as the preceding premise is fulfilled. Ideally, the distance should be in excess of 15 m.
- the identified flow path has been tested using conservative tracers before the onset of the sorbing tracer test.
- In order to answer up to the high safety and radiation protection standards applicable to Äspö HRL conditions, the mass recovery for conservative tracers in the flow paths considered should be at least in excess of 80%.
- It is assumed that the sink section to be employed in test set up will be selected on the basis of the Phase A test results, and that the source (injection) sections to be employed during Phase C will be selected on the basis of the results of the Phase B tests.
- It is assumed that the selected sink section also allows the possibility to carry out a sorbing tracer test in a known single structure. An advantage, but not a definite demand, is that the single structure is a component of the tested multi-component flow path mentioned above.
- It is identified as advantageous, but not imperative, if the tracer test layout, all other aspects considered, involve address of an identified fracture intersection.

With regards to the model predictions the following applies;

- No consideration to radioactive decay required. The experimental results will be compensated for decay, hence we can eliminate this effect.

## 4 Predictive approaches

In the following the predictive approaches listed in Section 2.3 are detailed. The approaches are;

- Stochastic continuum ENRESA/UPV/UPC
- Discrete Fracture Network NIREX/AEAT
- Channel Network JNC/Golder
- LaSAR SKB/KTH-WRE
- Posiva approach POSIVA/VTT

### 4.1 Stochastic continuum

#### 4.1.1 Objectives

The objective of the approach is characterising the spatially heterogeneous conductivities at the TRUE Block Scale site. This information is used as a way to obtain improved predictions on groundwater flow and contaminant mass transport. Multiple equally likely simulations of spatial heterogeneous hydraulic conductivities, all of which honour the experimental information (structural model, conductivity data, hydraulic heads at steady state, hydraulic heads from interference tests and tracer test information) are generated. The individual realisations characterise the spatial heterogeneity; also an ensemble average and variance can be obtained. The realisations which honour the experimental information are data charged and therefore provide more precise estimates with less uncertainty on groundwater flow and contaminant mass transport, than alternative unconditional realisations. Not only hydraulic conductivities, but also other parameters like storativities, prescribed heads along boundaries, dispersivity coefficients and porosity are calibrated.

#### 4.1.2 Basic assumptions and concepts

The groundwater flow at the TRUE Block Scale site is modelled assuming that both fracture planes and background fractures contribute to groundwater flow. This view can be justified by considering that background fractures (or non-detected fractures) may in fact participate in forming pathways. Therefore the groundwater flow model includes not only the deterministic structure planes, but also the background fracturing.

Furthermore, it is supposed that heterogeneity in hydraulic conductivity is an important characteristic of the site. Therefore, spatial variability in fracture plane and background hydraulic conductivity are modelled by geostatistical simulation methods.

The 3-D transient groundwater flow equation is solved with spatially variable hydraulic conductivities, i.e. the hydraulic conductivity changes from grid cell to grid cell. Also a storativity coefficient, estimated by given relationships between T and S in the literature, is assigned to the grid cells. Recharge and discharge can be considered, which may be variable in both space and time. As boundary conditions, prescribed head values, prescribed flux values or no flow conditions can be considered.

Mass transport is solved by the 3-D linear transport equation. The processes included are dispersion, diffusion, retardation, first order decay (radioactive decay), sink and sources and matrix diffusion. Matrix diffusion is considered by the hybrid integro-differential method (Galarza et al., 1990, Carrera et al., 1998). Matrix diffusion is solved analytically as a series of functions, truncation of this series and including the result as a sink/source term to the transport equation. Input parameters for the mass transport model are dispersivities, molecular diffusion, retardation coefficient, porosity, thickness, input concentration function and first order decay coefficient (radioactive decay). The hydraulic conductivities and boundary conditions are taken from the groundwater flow model. The heterogeneity of the conductivity field is fully retained, except some smoothing due to the differences in discretization between the flow and the transport model

The deterministic structure plane definitions provided by the reconciled March 99 structural model (Doe, in prep) are used to determine the grid cells that are intersected by the different fractures. Each cell is classified according to the structure that intersects it. In addition, cells not intersected by any structure plane are classified as background cells and cells intersected by more than one structure are classified as intersections. The planar extent of the fractures may, or may not be restricted within the model domain depending on the information on fracture plane limitations available.

#### **4.1.3 Implementation of the conceptual models**

The volume of groundwater flow model extends from 1790 to 2037 m Easting, from 7050 to 7277 m Northing and from -570 m to -283 masl. This volume is discretised in cubic grid cells of 6.66667 m size. A seven-point block centred finite differences algorithm is used for the solution of the flow equation. As part of performed scopings, numerical experiments have been necessary in order to get a solution as accurate as possible. Convergence problems in the solution of the linear system of equations occurred due to the large number of equations (N=54,094) and the high conductivity contrasts (especially between neighbouring background cells and fracture plane cells).



At the moment it is not clear whether for the conditioning to interference test data, a smaller simulation domain (and possibly a smaller grid cell size) will be used. In any case, the mentioned large simulation domain is used for the conditioning to conductivity data and steady state head data, while a smaller simulation domain will be used to model and calibrate the tracer tests.

The transport simulation domain extends from 1860 to 1960 m Easting, from 7130 to 7230 m Northing and from -520 to -420 masl. This area is discretized in about 10,000 finite elements of irregular shape, with large differences in size (the sides of the smallest one can be about 1 m, and the sides of the larger one near the boundaries can be about 20 m. However this is the first trial of the model, it can change due to numerical or conceptual requirements). Boundary conditions are taken from the larger scale groundwater flow model. Hydraulic conductivities are also taken from the flow model, but are downscaled to the finite element mesh of the transport model. In case the finite element is completely contained by a finite grid cell of the flow model, the hydraulic conductivity value of the finite element is the same as the hydraulic conductivity value of the grid cell. In case the finite element is contained by more than one grid cell of the flow model, a geometrical average is taken of the grid cell conductivities. The transport equation is solved by the numerical finite elements method.

Predicted is the spatio-temporal distribution of the concentrations. From this information also complete breakthrough curves of tracer test experiments can be obtained.

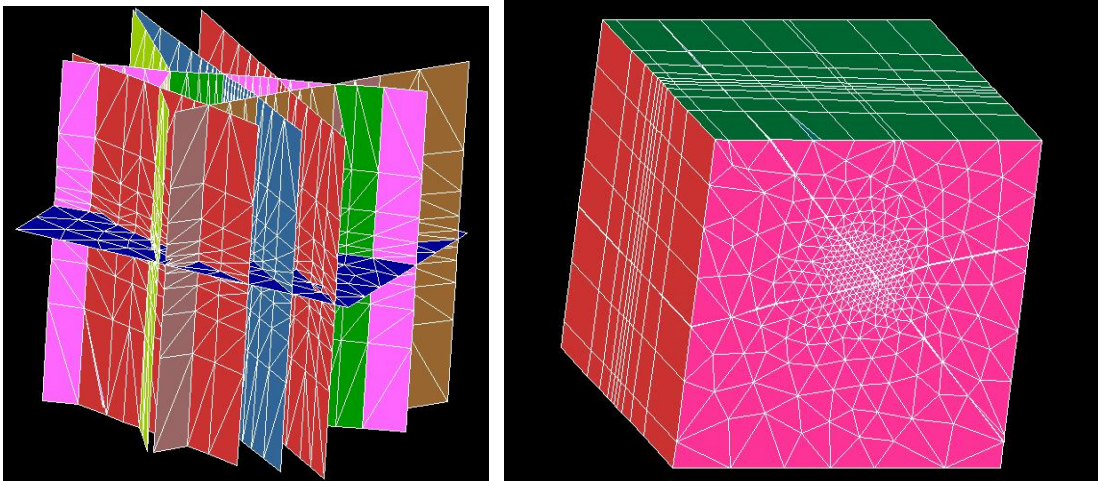


**Figure 4-1** Example of typical embedded 2D fracture and the associated 3D meshed planned to be used for transport calculations.

#### 4.1.4 Calibration to prior data

The sequential self calibrated method is adopted to incorporate prior information. The following information sources can be distinguished:

- Transmissivity data
- Steady state head data
- Interference test data
- Tracer test information

Independent transmissivity data sets are considered for each zone (background and each of the fracture planes) and consist of coordinates and measurement values. The data used are the estimated transmissivity values at the intersections of fracture planes and boreholes and the obtained transmissivity logs along the boreholes. Sequential simulation is used to incorporate the measurement values. The simulated hydraulic conductivities in each of the zones are conditioned to measurements taken in that specific zone. In case a grid cell belongs to more than one fracture plane (fracture intersection zone) the hydraulic conductivity at that grid cell is simulated for each of the fracture planes (using different conditioning data sets). The average of the simulated values is taken as the simulated hydraulic conductivity for the intersection grid cell. The variograms which should be used in the sequential simulation should be estimated from the experimental data. In case no reliable variogram estimation can be made, expert knowledge has to be used to adopt a variogram model.

The steady state head data set contains the measured head values at the different borehole sections. The sequential self calibrated algorithm, implemented in the computer code INVERTO, is used to condition the hydraulic conductivity simulations to the steady state head data. Decisions on the location and number of master blocks and the values of some optimisation parameters are taken after some preliminary tests. (The  $\log_{10} K$  perturbation field is parameterised as a function of the perturbation at a limited number of grid cells, called master blocks. The perturbations at locations other than the master block locations are obtained by interpolation of the latter, i.e., by ordinary kriging.). The variogram parameters which are used to interpolate the perturbations are the same as used in the sequential simulation. The perturbation at a grid cell is obtained by interpolating the perturbations at the master blocks belonging to the same zone as the grid cell. Remember that grid cells which are crossed by more than one fracture plane (fracture plane intersections) are located in a separate zone. INVERTO guarantees that at least a user-defined minimum number of master blocks are located in each zone.

The interference test data which are tried to be reproduced are the ones which test the connectivity of the structures which form the network where tracer tests are going to be carried out. Also for this conditioning process, the sequential self calibrated algorithm is used.

The inverse algorithm TRANSIN is used to condition to tracer test information. As indicated before, simulations with TRANSIN are carried out on a smaller domain with a different discretisation. The tracer test information is used to further improve the characterisation of the spatially heterogeneous conductivities and to calibrate porosity and dispersivity values. However, in order to condition on concentration data also prior estimates of various parameters have to be made. The prior estimate of the dispersivity coefficient depends on the distance between pumping and injection location and possibly the calibrated values from other tracer test experiments in the studied rock volume. The prior estimates of porosity and fracture equivalent aperture are made by taking into account information from literature, independent experiments and possibly calibrated values from other tracer tests in the studied rock volume. Prior estimates of input parameters for the matrix diffusion are made by information from the literature.

#### **4.1.5 Hypotheses testing**

The final result of the application of the inverse model is a series of conditional simulations, conditional to the structural model, hydraulic conductivity data, steady state head data, interference test data and tracer test data. The equally likely solutions give directly the answer to hypotheses 1 and 2 because they characterise the heterogeneity of the different fracture planes (including the new structures 21 and 22) and the fracture intersection zones (FIZ). The conductivity and heterogeneity of the fracture planes can be characterised by average, variance, probability distribution function etc. The same can be done for the FIZ. It can also be found out what is the discontinuity in hydraulic conductivity at the FIZ, whether the FIZ have in general a higher or lower hydraulic conductivity than the fracture planes, whether an important spatial heterogeneity in conductivity exists along one FIZ, etc. With respect to hypothesis 3, a different linear retardation coefficient can be assigned to every fracture and the matrix (it can also change inside each element, although it will not be the case in the first trials). In a FIZ, we superimpose two (or more) fractures, so we are implicitly modeling the effect of the intersection.

## **4.2 Discrete feature network**

### **4.2.1 Objectives**

The overall objective of the Nirex/AEA Technology approach is to build a sufficiently adequate ('real') model of the fracture system at the TRUE Block Volume using the discrete fracture network approach. The sufficiency of the model will be judged by the ability of the fracture network approach to be able to predict, reconcile or bound key characteristic features of groundwater flow and radionuclide as part of the Tracer Test Stage.

The specific objectives of the modelling are to:

- 1) describe the basic groundwater flow distribution in the key Structures (#13, #19, #20, #21, and #22);
- 2) estimate the dispersion characteristics of the breakthrough curves;
- 3) establish whether we can reconcile hydraulic, dilution tests and tracer transport characteristics;
- 4) predict the characteristics of a sorbing tracer test.

#### **4.2.2 Basic assumptions**

The basic assumption used in the discrete fracture network modelling to be performed by AEA Technology is that the reconciled March '99 structural model (Doe, 1999) defines the major structures which provide flow connections between injection and abstraction intervals for future tracer testing.

The discrete fracture network modelling will make no special assumptions regarding fracture intersections (i.e. providing enhanced flow paths). The most significant of the 'secondary' conductive features have been identified in boreholes, i.e. those inflows not correlated to the fractures identified in the March '99 model, using the differential flow logging techniques. It is conceivable that these 'secondary' or 'background' fractures are sufficiently important that they need to be accounted for when constructing the groundwater flow and transport model.

It is assumed that individual structures can be represented by variable aperture structures, with plausible geostatistical models being derived from a combination of generic and site specific information. For example, the following information will be considered when deciding on an appropriate model:

- Äspö fracture studies;
- Resin injection images from the Pilot Resin site (Hakami and Gale, 1999); and
- BIPS images taken from TRUE Block Scale site boreholes.

The above fracture data is expected to provide information on the variability of the fracture aperture on a short length-scale (typically on the 10's of centimetre length-scale, i.e. the dimensions of the borehole diameter). The interpretation of the likely internal structure of the fracture should be included, e.g. if the fracture shows any shear then an appropriate geostatistical model may be modified to include contact points (i.e. zero aperture).

The parameterisation of such models on a short length-scale and a larger integrated scale will be provided using a combination of transmissivity interpretations and dilution test interpretations. It is likely there will be significant disagreement between the transmissivity measured from the range of hydraulic tests (single-hole and cross-hole) performed in the studied block, and the dilution tests. However, the intention at this point is to try to avoid using a purely phenomenological approach that only predicts parameters you have initially estimated. For example, typically a phenomenological model requires fracture porosity and the dispersion length. These quantities are exactly the quantities the modelling is trying to predict (hence the tautology).

The apparent differences arising from the different forms of measurement and interpretation is not surprising, because the dilution tests are thought to test the local flow channels and hydraulic tests average over many flow channels. Therefore, the different testing is not expected to give the same effective properties without accounting for these different length scales. Figure 4-2 shows a schematic representation of a variable aperture fracture used to illustrate some of the key issues. Regions of enhanced porosity in which the flow is more stagnant determine the travel time in the fracture. However, the narrow channels control the overall conductivity of the fracture. The transmissivity estimates provided by the hydraulic test average over many flow channels and hence determine an averaged 'effective' aperture.

The first stage to the modelling is to decide on an appropriate geostatistical model and how it should be parameterised. In doing so, several practical difficulties need to be considered to ensure the differences are real, these include:

- The presence of multiple conductive fractures intersecting the borehole interval;
- The dilution test not sampling the average flux it is expected to be experiencing, given the transmissivity interpreted from the borehole. This discrepancy could possibly be due to near wellbore effects or that the borehole intersects a region in the tail of the aperture distribution.

Typically, an aperture based on the hydraulic tests alone give rise to a water travel time that is too short. Therefore, the models require more resistance of the groundwater flow without substantially changing the flowing volume. This may be introduced by either:

- incorporating large surface roughness with possible regions of zero aperture corresponding to fracture fill material or contact points due to fracture shear (the net results would be to increase tortuosity) with regions of enhanced porosity increasing the overall water travel time;
- multiple fractures that are in substantial contact.

It is likely that there will be some tracer tests with incomplete (<100%) recovery. These tests will fall into one of two categories. The first category includes those tests whose recovery would have been complete if the test had been carried on to completion. The second category include those tests in which tracer is lost to another sink. In the proposed modelling there is an implicit assumption that the lack of complete recovery of a conservative tracer can arise from two reasonable ‘process’ related sources:

- as a result of the background flow being sufficiently strong that tracer capture is incomplete or not possible;
- additional flow paths from the injection borehole are either weakly connected to the abstraction interval (it is expected this would give rise to a secondary peak in the tracer breakthrough if the tracer test could be taken to completion) or the injection borehole is not connected to the abstraction borehole at all. In which case tracer would not be recovered from the abstraction borehole.

It is conceivable that there is an additional reason for tracer ‘loss’ as a result of significant transverse dispersion. However, this is least likely in a convergent flow field.

The short travel time for conservative tracers should exclude significant diffusion in a direction transverse to the tracer stream tube (in the plane of the fracture) and therefore would not contribute to significant tracer loss. Experimental factors such as tracer failing to leave the injection interval, incomplete mixing in the injection borehole or the source and sink wellbore volumes being too large relative to the fracture volume, thus influencing the breakthrough characteristics of a tracer should be taken into account when evaluating tracer tests.

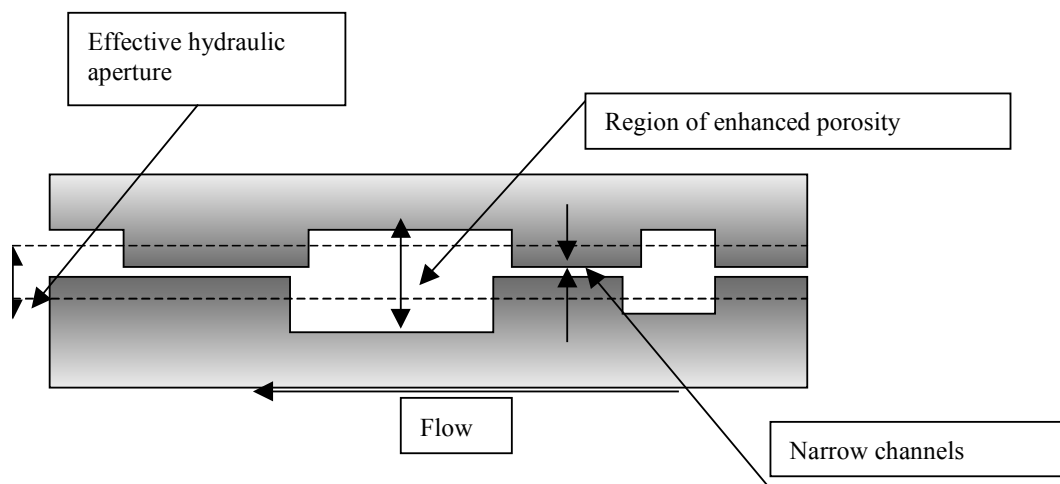


**Figure 4-2** A schematic representation of a variable aperture fracture. The regions of enhanced porosity in the fracture control the water travel time. The narrow channels control the overall conductivity of the fracture. The transmissivity estimates provided by the hydraulic tests average over many flow channels and hence determine an averaged ‘effective’ aperture.

### 4.2.3 Implementation

The discrete fracture network approach embodies the basic conceptual assumption that groundwater flow takes place predominantly in the fracture system in the TRUE Block Scale volume. AEA Technology proposes to use the discrete fracture network software NAPSAC, Hartley (1998) to model the key features in the TRUE Block Scale volume. The fracture network approach preserves the basic conceptual model of flow and transport confined to planar structures, and has the additional computational benefit of reducing the computational cost of simulations because the computations are performed in 2-D rather than 3-D.

The construction of the discrete fracture network model follows the basic philosophy embodied in the basic assumptions described in the previous section. The first basic steps are:

- 1) Construct a discrete fracture network model (geometrical model) based on the March '99 structural model including the key features. Because of this the detailed variability is anticipated to be on the sub (50m)<sup>3</sup> scale. The discretisation will reflect our desire to represent the variability on a short length-scale. The exact discretisation used in the modelling will be a balance between a desire to represent the geometry of variability and the computational costs. As the features will be represented as two-dimensional features we should be able to achieve a significant level of discretisation (perhaps on the 10's of centimetre scale) along the flow path. Discretisation can be easily modified once the flow path(s) for the planned tests with sorbing tracers have been identified.
- 2) Apply the boundary conditions developed by Holton, (1999) on the TRUE Block Scale volume;
- 3) Develop a spatial model (initially an isotropic geostatistical model in the fracture plane) of a variable aperture March '99 model that preserves as much as possible the small and larger scale variability observed;
- 4) Test the model against the various hydraulic, dilution and conservative tracer tests pertinent to the planned tracer test.
- 5) Calculate the transport for a particle released from the injection borehole using a rock matrix diffusion (and sorption) model (for the reactive tracers) using a standard Laplace transform algorithm, Hoch (1998);
- 6) Computations will be performed for several realisations to establish the statistical significance of the computed results.

To speed up the calculations it is anticipated that the Domain Decomposition method would be used in conjunction with an iterative method, Hartley (1998).

#### **4.2.4 Uncertainty**

The key uncertainties relating to the flow and transport will be accounted for using a combination of Monte Carlo simulations, as illustrated above, and parameter uncertainty. For example, parameter ranges will be estimated for the key sorption parameters from laboratory experiments.

#### **4.2.5 Calibration**

The basic model used to predict sorbing tracer transport begins with a groundwater flow model that has been run through Steps 1 to Step 4. The important calibration stages will need to give models that incorporate, as much as possible given the time-scale and budget constraints, the dilution test results, the pre-tests, and the Phase A and Phase B tracer tests. The results of this phase will give models that are able to describe the basic flow distribution in the fracture network and hence satisfy objective 1. A series of one-dimensional transport models (Hoch, 1998) are then computed based on the underlying flow model, this being parameterised using laboratory sorption estimates in preparation for the sorbing tracer prediction.

#### **4.2.6 Hypothesis testing**

The overall objective of the Nirex/AEA Technology approach is to build a sufficiently adequate ('real') model of the fracture system at the TRUE Block Scale volume using the discrete fracture network approach. The sufficiency of the model will be judged by the ability of the fracture network approach to be able to predict, reconcile or bound key characteristic features of groundwater flow and radionuclide as part of the Tracer Test Stage. The modelling is testing whether heterogeneity in the basic structural model is adequate to describe the results of the tracer testing, without introducing additional layers of complexity.

### **4.3 Channel network approach**

#### **4.3.1 Objectives**

JNC participates in the TRUE Block Scale experiment tracer transport modelling effort primarily to improve our understanding of radionuclide transport through networks of discrete fractures, and how this transport is different from transport within individual fractures. As a result, we are emphasising the factors which are different between fracture networks and individual fractures, and that is primarily in the effect of fracture intersections.



### 4.3.2 Background

The conductive fracture intensity indicated by Posiva flow logs and hydraulic test interpretations indicates a conductive fracture intensity of approximately  $P_{10} = 0.15 \text{ m}^{-1}$ , or 1 conductive fracture in 7 metres. Given the orientation distribution of background fractures, this corresponds to approximately 50 conductive (Posiva) discrete background features intersecting each of the deterministic Structures #13, #21, #22, and #20. This pattern of intersections may provide preferential channelling within the deterministic fracture planes, and it may be possible to look for these pathways in the deterministic features based on Posiva flow log data.

More central to this study, however, is the effect of the fracture intersections zones (FIZ) formed by the intersection of the major deterministic Structures #13, #21, #22, and #22. Most discrete fracture network (DFN) modelling assumes that the FIZ does not have a distinctive property. As a result, the primary flow element is the individual fracture, and the FIZ is treated only as a “mixing zone” for flow and transport between discrete fractures. This assumption has not been tested in situ, and as a result, remains one of the key issues for validation of the DFN approach in repository characterisation and performance assessment.

JNC wishes to address the issue as to whether the current treatment of FIZ in DFN models is appropriate, or whether a more sophisticated model is required. To determine this, JNC has decided to adopt a channel network modelling (CN) approach<sup>1)</sup>. In this approach, the 3-D discrete fracture network is transformed into a topologically equivalent network of 1-D channels. These channels provide conductivity, connectivity, and transport pathways equivalent to that provided by the planer elements of the DFN. However, since the CN model is based on a pipe concept, additional pipes can be included to represent the FIZ, with preferential flow or flow barrier properties. As a result, the CN model approach will allow JNC to assess the effects of FIZ on the ability of DFN models for flow and transport in fracture networks.

### 4.3.3 Model implementation

JNC’s approach for model implementation is described in three reports already prepared for the TRUE-Block Scale Project:

- Fox et al.(in prep) Evaluation of fracture and hydrological data to develop a stochastic/conditioned DFN
- Dershowitz et al. (in prep) Transformation of stochastic/conditioned DFN model to CN model for flow and transport, and
- Fox et al. (in prep) Prediction of Tracer Test PT-4 using calibrated/conditioned CN model.

This approach is summarised as follows.

1. The first step in model development is to develop the statistical and deterministic properties of the individual discrete features which are the basic building blocks of the fracture network. JNC/Golder will achieve this through a comprehensive analysis of fracture, hydraulic, and tracer data to build up the properties of the individual fractures #13, #21, #22, and #20 which are the focus of the predictive exercise, together with

<sup>1)</sup> In this context it is pointed out that the channel network approach presented above should not be confused with the “Channel Network Model” (CHAN3D) of Moreno and Neretnieks (1993), cf. eg. Gylling et al., (1998) for its application to the TRUE-1 experiments.

- the conductive background fractures as identified in the Posiva flow logs, and
- other deterministic (numbered) features which provide connections to boundary conditions established by the project.

This is achieved using JNC/Golder’s established techniques of spatial analysis, orientation and size analysis, and derivation of fracture transmissivity, storativity, channel flow width, and transport aperture. This produces a forward model of the TRUE Block Scale rock block.

2. The second step in model implementation is to take the model developed by the forward approach and apply it to model aggregate network behaviours of (a) hydraulic testing, (b) interference testing, (c) dilution testing, and (c) tracer testing. In this stage, a series of alternative hypotheses concerning network (FIZ) behaviour can be incorporated, and the key parameters which need to be adjusted to reproduce observed response can be established. The models are then adjusted as appropriate to remain consistent with measured data, and also with network. It is important to emphasise that this produces a range of models which are consistent to greater or lesser extents with particular aspects of the observed responses, rather than a single “true” model.

3. The range of models from step 2 can then be used to predict tracer tests results according to different hypotheses concerning key parameters and FIZ effects. The results of these predictions will be probabilistic, based on the relative likelihood of different parameter and assumption values. At the end, it is hoped that if the tracer test is designed carefully, it will be possible to distinguish the correct parameter values and the most reasonable FIZ assumptions.

#### **4.3.4 Calibration approach**

The JNC/Golder approach for model calibration will start with the conditioned/stochastic CN model developed for prediction of PT-4. This model will be updated

- for deterministic features of the structural model
- for conditioned features from the Posiva flow logs
- for stochastic features from BIPS and Posiva flow logs

This updating will be carried out based on

- updated fracture and hydrological information from new boreholes,
- interference and dilution testing results, and
- tracer test results from pre-tests, “Phase A” and “Phase B” tracer tests

The focus of this updating will be on understanding

- the specific transport pathways of concern for transport predictions, and
- connections to boundary conditions of concern for transport modelling

JNC/Golder model calibration is carried out as a systematic modification of the parameters which effect particular pathways, specifically modifying channel and FIZ properties of:

- geometry, through selection of different stochastic/conditioned background fracture and pipe generation realisations,
- pipe (channel and FIZ) flow properties of transmissivity and flow width, and
- pipe (channel and FIZ) transport properties of transport width and transport aperture.

The quality of the calibration is evaluated by comparison of the calibrated/conditioned model against in situ interference, tracer dilution, and tracer test responses.

#### **4.3.5 Prediction approach**

JNC/Golder’s primary purpose in this exercise is to learn about the properties of the FIZ, rather than to assume that we already know how FIZ effects flow and transport in fracture networks. As a result, JNC plans to prepare transport predictions using a range of conditioned CN models which reflect different assumptions concerning FIZ behaviour:

- FIZ serve only as mixing zones at fracture intersections
- FIZ properties are derived in the CN with distributions similar to other channels in the DFN
- FIZ properties are distinctly different, with for example higher transmissivity, higher aperture and lower flow and transport width.

One of these assumptions will be selected as the “reference” prediction. However, it is hoped that the results of transport modelling “Phase B” will make it possible to distinguish which of the above FIZ assumptions is most appropriate. This will be achieved by comparing transport along pathways which include FIZ, cross FIZ, and (presumably) do not include FIZ.

The number of model realisations feasible for the predictive phase will depend on the task budget and time limitations. As a result, JNC/Golder have not yet determined whether each of these predictions will be made as stochastic (probabilistic) or “best estimate” predictions.

#### **4.3.6 Evaluation approach**

JNC/Golder propose to evaluate tracer breakthrough by two approaches:

- comparison of overall breakthrough predictions and measurements in terms of  $t_{50}$ , % recovery, and breakthrough curve shape, and
- comparison of back calculated properties of pipes along the pathways tested by conservative and sorbing tracers, i.e.,

The comparison of back calculated pipe properties will be expressed in terms of

- path lengths
- transport apertures, and
- transport widths

It is hoped that this evaluation will allow us to distinguish whether particular pathways exhibit differences between conservative and sorbing tracer breakthrough which might be indicative of FIZ effects, either as a result of

- particular FIZ hypothesis models providing more robust predictions, or
- back calculated pathway properties more consistent with particular FIZ hypotheses.

#### **4.3.7 Approach to conceptual and parametric uncertainty**

JNC/Golder are concerned with conceptual uncertainty regarding alternative FIZ hypotheses, and also parametric uncertainty of transport pathways.

Although JNC/Golder does not expect the TRUE-BS experiment to resolve conceptual uncertainty regarding alternative FIZ hypotheses, we do hope that this experiment will provide some insight. In order to achieve this, we expect to implement models which reflect extremes of alternative assumptions concerning FIZ effects, and to use these models for both calibration and predictive exercises. Perhaps the models which perform best will provide an indication toward reducing this underlying conceptual uncertainty.

JNC/Golder does not consider the issue of matrix diffusion and sorption to be an issue of conceptual uncertainty but rather a matter of established physics, with physically based parameters such as free water diffusion, distribution coefficients  $K_a$  and  $K_d$ , and porosities. There is, however, parametric uncertainty for a number of parameters including flow and transport channel widths, immobile and mobile zone properties, and dispersion coefficients. These uncertainties will be addressed through sensitivity studies to establish the range of parameters consistent with field observations.

JNC also considers uncertainties in pathway geometry due to the uncertain aperture structure within fracture planes and also due to the presence of background fracturing and possible FIZ structures. This uncertainty may be addressed through the use of Monte Carlo (stochastic) simulation if time permits.

### **4.4 SKB/KTH-WRE LaSAR approach**

#### **4.4.1 Objectives**

#### **4.4.2 Basic concepts**

The LaSAR (Lagrangian Stochastic Advection-Reaction) approach for a single fracture used in the prediction and evaluation of the results of the TRUE-1 experiments is extended to the TRUE Block Scale experiments. The transport flow path in which tracer experiments are conducted is conceptualized as a number of single fractures (Figures A4-1 and A4-2), connected serially (head-to-tail). Each single fracture is approximated as a two-dimensional planar fracture with spatially variable aperture. Each fracture has a different aperture statistics. There can be mass losses at the connection of fractures. A solute is injected into the fracture, it is advectively transported by the bulk water and is dispersed due to velocity variation. It is also subject to various mass transfer processes. These processes are; diffusion into rock matrix, sorption in the matrix, diffusion into stagnant water, sorption on fracture surfaces, and sorption onto gouge material.

Fluid flow in the fracture is two dimensional and is random due to the random variation of the fracture aperture. The flow will be determined by the variable aperture and the boundary conditions. The advective flow field is solved using Monte-Carlo simulations by a standard, commercially available code (MODFLOW, 1994). Transport is solved in two steps. In the first step, the joint distribution of  $\beta$  and  $\tau$  is obtained by particle tracking in the flow field using Monte-Carlo simulations. In the second step, the analytical solution for each individual mass transfer process for a pulse injection is obtained by the method of Laplace transforms. The solution for coupled processes is obtained by convolution of the solution of each individual process. The solution for continuous input is obtained by convolution of the continuous input function and the solution for pulse input. Dispersion effects are accounted for by integration over  $\beta$  and  $\tau$  along random flow paths.

#### 4.4.3 Basic assumptions

The following assumptions are made:

- The flow is assumed to be steady state;
- The tracer is transported only advectively in the fracture;
- The tracers are fully mixed in the fracture, in the direction orthogonal to the fracture plane;
- The advective transport in the rock matrix is negligible. The tracer only diffuses into the rock matrix in the direction orthogonal to the fracture plane, i.e., diffusion into the rock matrix is one dimensional;
- All mass transfer processes are linear;
- The sorption on the inner surfaces of the rock matrix is assumed to be at equilibrium;
- The sorption on the fracture surfaces is also assumed to be at equilibrium;
- The sorption onto gouge material is assumed to be first-order kinetically reversible;
- The matrix porosity  $\theta$  and the diffusivity  $D$  in the rock matrix are assumed to be spatially uniform.

#### 4.4.4 Key parameters and prediction procedure

The generalized key parameters in the LaSAR framework are  $B_a = \sum_{i=1}^N K_{ai}\beta_i$  for surface sorption, and  $B = \sum_{i=1}^N \kappa_i\beta_i$  for diffusion/sorption in the rock matrix.  $K_{ai}$  is the distribution coefficient for surface sorption (which is assumed to be at equilibrium), and  $\kappa_i = \theta_i [D_i(1 + (K_d^m)_i)]^{1/2}$  is the parameter for diffusion/sorption in the rock matrix. Here the subscript  $i$  denotes parameters in the  $i$ th fracture.  $\theta_i$  is the porosity of the rock

matrix,  $D_i$  is the pore diffusivity in the rock matrix ( $\theta_i D_i$  is the effective diffusion coefficient in the rock matrix), and  $K_{di}^m$  is the sorption coefficient in the rock matrix.  $\theta_i$ ,  $D_i$  and  $(K_d^m)_i$  are in principle all to be determined in the laboratory. Our evaluation results for the detail scale TRUE-1 experiments indicate that the laboratory value of  $\kappa_i$  may not be applicable in the field. A calibration of  $\kappa_i$  may be required for the field value. Our working hypothesis is that  $\kappa_i$  and  $K_{ai}$  are *uniform* and *constant* for all fractures. Then  $B = \kappa\beta$  and  $B_a = K_a\beta$ , where  $\beta \equiv \sum_{i=1}^N \beta_i$  and  $\kappa$  and  $K_a$  are the constant values.

Two additional parameters considered in the LaSAR framework are the distribution coefficient for the sorption onto gouge material,  $K_d^g$  (once equilibrium has been reached), and a backward rate coefficient  $\alpha$ . Laboratory values of  $K_d^g$  and  $\alpha$  are not available. They need to be inferred entirely from the measured breakthrough data.

There are two steps in the prediction procedure:

(1) We determine the joint distribution of  $\beta$  and  $\tau$ . The joint distribution of  $\beta$  and  $\tau$  may be obtained using Monte-Carlo simulations through particle tracking. An alternative method is to find an approximate relationship between  $\beta$  and  $\tau$  (e.g., linear relationship,

Cvetkovic et al, in preparation; power law relationship, Cvetkovic et al, 1999) and to assume the distribution of  $\tau$  by an analytical form  $g(\tau)$  (e.g., Inverse-Gaussian, Cvetkovic et al, in press). The moments of  $g(\tau)$  are obtained by deconvolution from the experimental breakthrough data of non-reactive tracers while accounting for the diffusion into the rock matrix. In other words, we need to find the moments of  $g(\tau)$  that match the predicted breakthrough values with the experimental breakthrough data.

(2) We use  $g(\tau, \beta)$  or  $g(\tau)$  to predict the breakthrough curves of reactive tracers by considering all the mass transfer processes with the parameters either directly determined in the laboratory or calibrated with factors found in the TRUE-1 evaluation (Cvetkovic et al, in press).

## 4.5 POSIVA/VTT approach

### 4.5.1 Objectives

Objective of the approach is to predict the tracer breakthrough using mainly the flow rate information from the dilution tests.

### **4.5.2 Overview of approach**

It is estimated that the main retardation process taking place under natural flow conditions from the deep underground repository is matrix diffusion. In this case the interaction between the migrating species and surrounding rock is controlled, not only by the retardation and diffusion properties of the rock matrix, but is also governed by the flow rate over unit width of the flow channel (and, of course, on the length of the flow path). Matrix diffusion- like behaviour is possible in relation to the stagnant areas of the flow field or fault gauge. In this approach the breakthrough of the tracer is predicted using the flow rate information from the tracer tests and dilution tests.

The approach is not valid if the major process of transport is pure advection. Additional studies are conducted using, for example the discrete fracture network approach, to get realistic view on the distribution of the flow rate along the flow channels. The relationship between the transport and hydraulic apertures is taken from the TRUE Block Scale tracer tests performed thus far, or from the experience from the TRUE-1 tracer tests.

### **4.5.3 Basic assumptions and concepts**

Transport from the source area to the sink takes place along the streamlines that are crossing the source area. If the major part of the streamlines do not end at the sink, then the recovery of the tracer test will not be very high. Let us assume that all the streamlines starting from the source goes to the sink. All these streamlines which cross the source area form a streamtube.

If the flow rate at the source area caused by the sink is high then tracer transport is dominated by the advective field in the streamtube. This means that the mean breakthrough time is controlled by the mean transport aperture along the streamtube. The dispersion is controlled by differences in breakthrough time along different streamlines.

If the flow rate is decreased, the molecular diffusion becomes a more important process. By molecular diffusion it is possible that the tracer molecules can visit other streamlines inside or outside the streamtube and also other water-filled areas, e.g. the pore space of the rock matrix. The first effect which takes place when the flow rate is decreased, is the mixing of the tracer across the streamlines of the streamtube. This causes a Taylor-like dispersion effect in the breakthrough curve. Taking molecular diffusion into account may even diminish the dispersion of the breakthrough curve because the tracer particles have an opportunity to "integrate" transport time along different streamlines of the streamtube.

If the flow rate is further decreased, then the diffusion between the streamtube and the surrounding environment start to become important. This surrounding environment may be stagnant areas of the flow field i.e. some areas in the flow channel just beside the streamlines of the streamtube or it may also the stagnant pore space of the rock matrix or fault gauge.



The analytical solution for the flow along a fracture and diffusion into the pore space of the surrounding rock shows that the retention due to the matrix diffusion is depending on the flow rate across unit width of the flow channel. In the tracer test the flow channel is determined by the streamtube starting from the source area. As a first guess the flow rate across the unit width of the flow channel is set to the total flow rate across source area divided by the width of the source area.

If the flow rate is small enough, the retardation by matrix diffusion fully dominates the breakthrough so that even the transit time along the advective field can be neglected when the breakthrough is estimated.

#### **4.5.4 Prediction approach**

In a tracer test the flow rates are usually such that the breakthrough is dominated by the advective field and the dispersion by the advective field together with the molecular diffusion in the streamtube. This means that the mean breakthrough time cannot be estimated using the flow rate only. Therefore, following procedure will be applied to estimate the breakthrough:

- The streamtube from the source area to the sink is replaced by a flow channel
- The flow rate along the channel is taken from the tracer test data. The length of the flow channel is estimated using DFN simulations. DFN simulations are also used to study the variation in the width of the flow channel because strictly the parameter controlling the matrix diffusion effect is the integral of the width of the flow channel along the flow path.
- The relationship between the hydraulic and the transport aperture may be calibrated using tracer test data from the TRUE Block Scale site or from the TRUE 1 site.
- The shape of the advective field in the flow channel is assumed to be linear. Molecular diffusion in the flow channel is taken into account. The actual shape of the advective field in the flow channel is not important because the molecular diffusion smoothens it.
- interaction between the migrating tracer and the stagnant areas of the flow field, fault gouge and rock matrix are taken into account by using an analytical approach and the flow rate along the flow channel.



## **5. Common assumptions**

The common assumptions are divided into two basic groupings, one which is related to the basic geometrical model, its information in terms of a calibration data set made up of a) available material property data, b) drawdown and breakthrough data from hydraulic and tracer tests (up till the onset of the Phase C tests with sorbing tracers), and c) head boundary conditions. The second grouping is an account of the uncertainties, geometric and parametric which are related to the calibration data set.

### **5.1 Conductive geometry**

The most recent structural model (March'99) presented by Hermanson (in prep) has been reconciled by Doe (in prep) using available drilling, single hole and multiple hole interference test data and tracer dilution data. The basic result of the reconciliation is some minor adjustments to the extents of some of the key target structures (Structures #13, #21 and #22). The fourth, and major component of the studied fracture network, is Structure #20, cf. Figure 5-1.

During early Autumn 1999, an additional borehole (KI0025F03) has been drilled, oriented in between KI0025F02 and KI0023B. The characterisation of the borehole is still ongoing but the borehole has tentatively provided verification to the reconciled structural model and interpreted deterministic structures (#5, 6, 7, 13, 20, 21 and 22).

It is foreseen that that the predictions of the tests with sorbing tracer tests will be carried out using a structural model which will be informed both with the characterisation data from KI0025F03, and the results of the Phase A tests.

### **5.2 Calibration data set**

#### **5.2.1 Material properties**

Transmissivity data has been collected from the exploration boreholes using different techniques, and at various scales. Steady state estimates of transmissivities on a 5 m support scale has been obtained from some of the earlier boreholes (Gentzschein, 1997a, 1997b, 1998). These tests were followed by transient flow and pressure build up tests in selected sections, primarily located in potential target structures of bounding structures

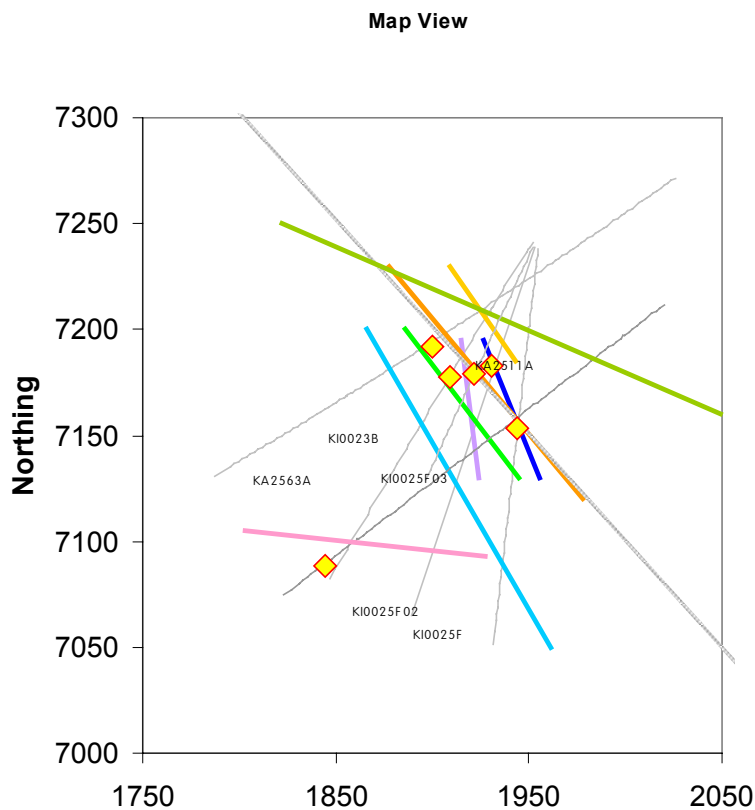


**Figure 5-1** Reconciled March '99 Structural model including the trace of the new borehole KI0025F03. The shown deterministic structures with their interpreted extents are : Red = Structure #20, Light green = Structure #13, Violet = Feature #21, Dark Blue = Feature #22, Yellow = Structure #6, Light blue = Structure #19, Dark green = Structure #7, Pink = Structure #10.

(Gentzschein and Morosini (1998), Adams (1998) and Adams et al, (1999), Doe and Fox (in prep)). The latter evaluations also include estimates of specific storage and skin. Estimates from crosshole interference tests, assumed valid over a larger volume, are also available (Andersson, et al (1998), Adams et al., (1999) and Andersson et al. (1999), Andersson and Ludvigsson (2000)).

Doe (in prep) have tabulated the transmissivities from various sources associated with the interpreted deterministic structures at each intercept. In addition, a best estimate of the transmissivity at each interpreted borehole intercept is provided.

### **5.2.2 Drawdown data**

Two types of drawdown data are available; drawdown due to drilling and drawdown from controlled cross-hole interference tests. The former data set has been a vital component in establishing connectivity and reconciling the most recent structural model (Doe, in prep, a). However, for the purpose of calibrating the models to be employed for predictive modelling the crosshole interference data sets will be used. The data sets considered are the Spring 1998 crosshole interference tests (Andersson et al., 1998), the results of the combined cross-hole interference, buildup and tracer dilution tests in KI0025F02 (Adams et al., in prep), KI0023B and KI0025F02 and KI0023B (Andersson and Ludvigsson, 2000) and the Spring 1999 Pre-tests (Andersson, et al, 1999)).

Additional data will emerge from the hydraulic parts of the Phase A and Phase B tests are foreseen. This includes highly controlled interference tests using selected sink sections in our target structures. This data set will also be used to assess possible hydraulic boundaries.

### **5.2.3 Tracer dilution data**

Tracer dilution data at ambient undisturbed conditions and at pumped conditions have been collected with the objective of identifying suitable injection points for tracer in the studied fracture network (Andersson, et al., 1998, Adams, et al., 1999, Andersson and Ludvigsson, 2000, Andersson et al., 1999). This data set may potentially be used as calibration data, but it should be realised that the data are totally governed by the local transmissivity (and gradient) at the point of measurement. The test campaigns during which tracer dilution data have been collected are described in Section 5.2.2.

Additional tracer dilution test data, using alternate sink sections, primarily collected with sinks established in the new borehole KI0025F03 will be performed within the context of the Phase A tests. Tentatively, some 30 tests, both at ambient and stressed conditions, will be performed using 4 different sink sections.

### **5.2.4 Tracer breakthrough data**

Tracer breakthrough data have been collected from two tests, the ESV-1c test (part of Spring 1998 tests) (Andersson et al., 1998) and from the PT-4 test (part of Spring 1999 Pre-tests) (Andersson, et al., 1999). Altogether five breakthroughs have been obtained, whereof four show significant recoveries, and one, obtained over a large distance, show a very low recovery.

It is foreseen that additional breakthrough data will become available from;

- Phase A tests : one sink, max 4 injections
- Phase B tests : one sink, number of injections not defined at present

## **5.3 Boundary conditions**

Basic boundary conditions are available for extraction from a site scale DFN model which has been updated to also include structures interpreted in the TRUE Block Scale volume (Holton, 1999). This model has been compared to field data (inflow to tunnel segments) and to a corresponding continuum model (Svensson, 1997) calibrated to available head data from borehole sections.

In order to provide support for the modelling teams in mapping changes in boundary conditions over time in their assignment of boundary conditions, a number of plane view head maps over the TRUE Block Scale rock volume will be produced, related to the time period during which major tests have been conducted. The following time periods have been selected;

- Spring 1998
- September 1998
- May 1999
- October 1999
- Autumn 2000

## **5.4 Common uncertainties**

The identified common uncertainties are associated conceptual and parametric uncertainty. To the first grouping belong the uncertainties associated with the geometrical (structural) model. To the second group belongs uncertainties associated with transmissivity and its distribution in space and uncertainties associated with collected drawdown data and breakthrough data.

### **5.4.1 Conceptual uncertainty**

The developed structural model constitutes a hypothesis in itself which is subject to testing during the various hydraulic and tracer tests. The present structural model (Doe, in prep) is considered to be satisfactorily known to warrant continuation of the planned tracer test programme. However, there is still a degree of uncertainty related to the identified target fracture network. This uncertainty can be divided into a) the complexity and extent of the identified structures is not known in full, b) there may still be structures which may play a part in the planned tracer tests. These are primarily assumed to belong to the background fracture population.

In the reduction of data related to individual structures, intersection data on a given structure from various boreholes are fitted to a least square fit plane. In doing so, and when implementing the simplified planar structure in a numerical model, an error is introduced. This error can be managed by making subtle changes to the packer positions in the numerical models such that a consistency is attained between the modelled packer positions and the structures they are supposed to pack off. A list of such virtual packer positions with a corresponding list of actual packer positions will be prepared as part of the Phase A work.

## 5.4.2 Parametric uncertainty

### *Transmissivity*

The parametric uncertainty associated with transmissivity is governed by the underlying uncertainty in measurement of flow, pressure and the packer spacing (*Instrument uncertainty*). The pressure is measured with an accuracy of  $\pm 0.1\%$  of full scale (5 MPa) whereas the uncertainty in flow determination vary depending on the technique used. In the case of flow and pressure build-up test using the UHT-1 equipment (flow and pressure build-up tests) the uncertainty is  $\pm 0.4\%$  of the actual flow rate in the interval 0-1 kg/min (small flow meter, zero stability =  $\pm 1\text{E-}4$  kg/min) and  $\pm 0.15\%$  of the actual flow rate in the interval 0-100 kg/min (large flow meter, zero stability =  $\pm 3\text{E-}3$  kg/min)

In the case of interference tests in conjunction with tracer dilution tests, the accuracy in the manual flow determination is estimated at  $\pm 5\%$ . In the case of automatic regulation the uncertainty is  $\pm 0.4\%$  in the interval (1-5 kg/min, zero stability =  $8\text{E-}4$  kg/min. The accuracy in the POSIVA flow logging is  $\pm 10\%$  of the currently measured value in the measured range 2-5000 ml/min .

To these discrete errors should be added those which are associated with flow regulation (maintaining a constant head/or flow rate) (*Test procedure uncertainty*). In both cases the error is estimated to 2% of the actual value. The error in regulation to a given dp is estimated to be  $<1\%$ . However, the error at low dp:s in determination of initial absolute pressure can be as high as 20%. Compliance effects can result in an error of 20% of the minimum flow, dependent of the selected minimum flow rate In the transmissivity range tested at the TRUE Block Scale site the latter uncertainty is estimated to be  $\pm 3-45\%$

The overruling source of uncertainty, however, is introduced by the selection of the proper interpretation model (*Conceptual flow model uncertainty*). The selection of flow model, although effective diagnostic tools are available, is to large extent subjective. In the case an improper flow model has been selected, the uncertainty can be one to two orders of magnitude. Here, we assume that a proper flow model (and segment of the test curve) has been selected on the basis of suitable diagnostics. The remaining uncertainty which is introduced in the actual interpretation and curve fitting (*Interpretation uncertainty*) Under the above assumptions the interpretation uncertainty is estimated to be in the order of 5%.

In total the uncertainty associated with a transmissivity determination in the range  $10^{-9}$  to  $10^{-4}$  m<sup>2</sup>/s is estimated to be less than  $\pm 50\%$ , this figure valid for a low transmissivity and a low dp. In the case of a more transmissive section the uncertainty can be much less.

#### *Drawdown*

The drawdown in terms of head are calculated using information about the absolute pressure, the elevations of the test section and pressure transducer, the salinity of the water in the tubings connecting the section to the surface. Since drawdown is the difference between an initial head and head at pumped conditions (evolving with time) the errors are effectively cancelled out. However, as in the case with the hydraulic tests the determination of the reference head or level can be associated with an uncertainty as large as 20%.

#### *Concentration*

The concentrations of measured conservative metal complex tracers are associated with an uncertainty of measured within  $\pm 3\%$ . Similarly the concentrations of fluorescent dye traces are within  $\pm 1\%$ .

In the case of gamma-spectrometric measurements the uncertainty in an individual measurement is assumed to be  $<5\%$ . The actual measurement is however dependent on the time over which the measurement is made, the initial activity of the radioactive compound injected, and the choice of radioactive isotope. It is envisaged that at low activity and short measurement times the uncertainty can be as high as  $\pm 50\%$ , in the case of individual measurements.

#### *Transport parameters from the laboratory*

Uncertainties associated with determinations of diffusivities and distribution coefficients are reported by Byegård et al. (1998).



## **6. Concluding remarks**

The present report presents a number of approaches which uses various ways to integrate the assembled site-characterisation data. They also have their own respective agendas and approach-related hypotheses to test. The techniques range from full 3D numerical schemes to reductions of the problem to 2D and 1D analytical transport frameworks, the latter supported in varying degree by numerical flow modelling.

Beyond the account of the different approaches presented herein, it is beyond the scope of this report to evaluate the concepts relative to on another. In the subsequent evaluation of the predictive work, the inherent similarities and differences will be highlighted and discussed.



## 7. References

**Adams, J. 1998** : Preliminary results of selective pressure build-up tests in borehole KI0023B. Swedish Nuclear Fuel and Waste Management Co. Äspö Hard Rock Laboratory International Progress Report IPR-01-43.

**Adams, J., Andersson, P., Meier, P. 1999** : Preliminary results of selective pressure build-up tests in borehole KI0025F02. Swedish Nuclear Fuel and Waste Management Co. Äspö Hard Rock Laboratory, International Progress Report IPR-01-56.

**Andersson, P., Ludvigson, J-E., and Wass, E. 1998** : Combined interference tests and tracer tests. Swedish Nuclear Fuel and Waste Management Co. Äspö Hard Rock Laboratory International Progress Report IPR-01-44.

**Andersson, P., Ludvigsson, J-E., Wass, E., and Holmqvist, M. 1999** : Interference tests and tracer tests PT-1 – PT-4. TRUE Block Scale Project, Detailed Characterisation Stage. SKB Äspö Hard Rock Laboratory, International Progress Report IPR-01-52.

**Andersson, P. and Ludvigsson, J-E. 2000** : Tracer dilution tests during pumping in borehole KI0023B and short-term interference tests in KI0025F02 and KA31510A. . TRUE Block Scale Project, Detailed Characterisation Stage. SKB Äspö Hard Rock Laboratory, International Progress Report IPR-01-57.

**Byegård, J., Johansson, H., Skålberg, M., and Tullborg, E-L. 1998** : The interaction of sorbing and non-sorbing tracers with different Äspö rock types. Sorption and diffusion experiments in the laboratory scale. . Swedish Nuclear Fuel and Waste Management Co. SKB Technical Report TR-99-18.

**Carrera, J., X. Sánchez-Vila, I. Benet, A. Medina, G. Galarza and J. Guimerà 1998** : On matrix diffusion: formulations, solution methods and qualitative effects. Hydrogeology Journal. 6 (2), pp. 178-190.

**Cvetkovic, V., Selroos, J.-O., and Cheng, H. 1999** : Transport of reactive tracers in rock fractures, J. Fluid Mech., 378, 335-356.

**Cvetkovic, V., H. Cheng and J.O. Selroos, (in press)** : Evaluation of TRUE-1 sorbing tracer experiments at Äspö: Theory and applications, SKB International Cooperation Report .

**Doe, T. 1999** : Reconciliation of the March'99 structural model and hydraulic data. Swedish Nuclear Fuel and Waste Management Co. Äspö Hard Rock Laboratory International Progress Report IPR-01-53.

**Doe, T. and Fox, A. (in prep)** : Flow dimension analyses of pressure buildup tests from borehole KI0025F02. Swedish Nuclear Fuel and Waste Management Company, Internal Report.

**Galarza, G., J. Carrera and A. Medina 1990** : Implementacion numerica de la difusion en la matriz dentro de un modelo matemático de la ecuación de transporte. Proc. del I Congreso de Metodos Numericos. Ed. SEMNI, pp. 541-549.

**Gentzschein, B. 1997a** : Detailed flow logging of core borehole KA2563A. Swedish Nuclear Fuel and Waste Management Co, Internal Report.

**Gentzschein, B. 1997b**: Detailed flow logging of core boreholes KA2511A, KI0025F and KA3510A using a double packer system. Swedish Nuclear Fuel and Waste Management Co. Äspö Hard Rock Laboratory International Progress Report IPR-01-69.

**Gentzschein, B. 1998** : Detailed flow logging of core borehole KI0023B using a double packer system. Swedish Nuclear Fuel and Waste Management Co, Internal Report.

**Gentzschein, B. and Morosini, M. 1998** : Selective pressure build-up tests in borehole KI0023B. Swedish Nuclear Fuel and Waste Management Co. Äspö Hard Rock Laboratory International Progress Report IPR-01-45.

**Gylling, B., Khademi, B., Moreno, L. 1998** : Modelling of the Tracer Retention Understanding Experiment Task 4C-D using the channel network approach. SKB Äspö Hard Rock Laboratory, International Cooperation Report ICR 98-01.

**Hakami, E. And Gale, J. 1999** : First TRUE Stage pilot resin experiment – Pore space analysis. SKB Äspö Hard Rock Laboratory, International Progress Report IPR-99-14.

**Hartley L, 1998**. NAPSAC (Release 4.1) Technical Summary Document, AEA Technology Report AEA-D&R-0271.

**Hermanson, J. (in prep)** : March 1999 Structural model – Update using characterisation data from KI0025F02, KA3600F and KA3573A. Swedish Nuclear Fuel and Waste Management Co., Internal Report.

**Hoch, A. R. 1998** Implementation of a rock-matrix Diffusion Model in the Discrete Fracture Network Code NAPSAC, Nirex Science Report S/98/005.

**Holton, D., 1999** : Boundary Conditions for sub-models at the Äspö TRUE Block Scale Site. Äspö Hard Rock Laboratory, International Progress Report IPR-01-50, TRUE Block Scale Project Swedish Nuclear Fuel and Waste Management Co., SKB, Stockholm, Sweden.

**MODFLOW/EM**, The USGS Three Dimensional Ground Water Flow Model, MaximalEngineering Software, Inc, 1994.

**Moreno, L. and Neretnieks, I. 1993** : Fluid flow and solute transport in a network of channels, J. of Cont. Hydrology, v. 14, pp. 163-192.

**Svensson, U. 1997** : A site scale analysis of groundwater flow and salinity distribution in the Äspö area. . Swedish Nuclear Fuel and Waste Management Co, Technical Report TR-97-17.

**Winberg, A. (ed.) (in press)** : Final Report of the Detailed Characterisation Stage – Compilation of premises and outline of programme for tracer tests in the block scale. SKB Äspö Hard Rock Laboratory, International Progress Report IPR-00-26.

**Winberg, A. 1997** : Test plan for the TRUE Block Scale Experiment. Swedish Nuclear Fuel and Waste Management Co. Äspö Hard Rock Laboratory International Cooperation Report ICR 97-02.

**Winberg, A. et al. 2000** : Final Report of the First Stage of the Tracer Retention Understanding Experiments. Swedish Nuclear Fuel and Waste Management Co, Technical Report TR-00-07.



**Table 1-1 ENRESA - Breakdown of flow model used in predictive modelling**

Basic assumptions	Conceptual model and its geometrical representation	Input parameters (spatial model)	Model size	Discretisation	Numerical solution
<p>Background also important Heterogeneity in background and fracture planes. Data are used by SSC for improving representation of heterogeneity mapped by characterisation.</p>	<p>Grid cells belong to different zones (background or fracture planes).</p>	<p><math>K(x,y,z)</math> from geostatistical simulation. Boundary conditions from regional groundwater flow model (prescribed heads or flow).  Storativity information from interference tests.</p>	<p>Easting : 1790-2037 m, Northing : 7050-7277 m Elevation : -570 to - 283 masl</p>	<p>37 x 34 x 43 cubic cells (Length of cell sides =6.66667 m</p>	<p>Seven-point block centred finite difference method</p>

**Table 1-2 AEAT - Breakdown of flow model used in predictive modelling**

Basic assumptions	Conceptual model and its geometrical representation	Input parameters (spatial model)	Calibration/ prediction	Discretisation	Numerical solution
<p>The basic assumption is that groundwater flow and transport take place on fracture planes.</p>	<p>The basic conceptual model is that of a Discrete Fracture Network (DFN) in which the heterogeneity is represented as variable aperture fractures. The basic model being a parameterised March '99 structural model.</p>	<p>An isotropic spatial model with a representation of the small-scale variability and perhaps a larger scale spatial model. The larger scale model will be constructed from the identified transmissivity of the named features. Any smaller scale variability (flow channels) will be estimated from the dilution tests. Soft data such as the BIPS and resin injection data from TRUE-1 will be used as a check to see if the kind of variability that has been selected is reasonable. In particular, attention will be given to whether the fracture has additional porosity / or structure. This would be an extra check if the introduction of extra porosity were justified when 'calibrating' breakthrough curves.</p>	<p>Before prediction of the sorbing tracer test a calibrated flow model will be constructed. This calibrated model will use the relevant pre-testing results, the Phase A and Phase B results (head, and dilution characteristics) for predictions of: Head (drawdown, not already calibrated) Dilution (not already calibrated).</p>	<p>The discretisation should reflect our desire to represent the variability on a short length-scale to account for the small-scale variability. As the features will be represented as two-dimensional features we should be able to achieve a significant level of discretisation. It is hoped 10 to 100 realisations would be calculated to establish the necessary spread in the computed results.</p>	<p>To speed up the calculations it is anticipated that the Domain Decomposition method will be used in conjunction with an iterative method.</p>



**Table 1-3 JNC/Golder - Breakdown of flow model used in predictive modelling**

Basic assumptions	Conceptual model and its geometrical representation	Input parameters (spatial model)	Model size	Discretisation	Numerical solution
<p>The basic assumption is that groundwater flow in the fracture network of interest can be approximated using constant density, single porosity, laminar flow assumptions. Flow and transport are assumed to occur primarily on channel pathways within fracture planes.</p>	<p>The basic conceptual model is that of a Discrete Fracture Network (DFN) in which the flow and transport pathways are represented as channel (CN) connections between and along fracture intersections</p>	<p>The underlying DFN model is described by deterministic features, and stochastic/conditioned features defined by distributions of location, size, shape, and orientation. The channel network is defined by assumptions relating the channel network geometry to the fractures and fracture intersections.</p>	<p>The model extends to the boundaries of the model region (500m) with greater detail in the area focused on Structures #13, #20, #21, and #22.</p>	<p>The model is discretized to the scale of an individual pipe between, or along fracture intersections. These vary in scale from on the order of 0.1 to 10m.</p>	<p>Flow is solved by Galerkin finite elements using a conjugate gradient solver.</p>

**Table 1-4 SKB/LaSAR -Breakdown of flow model used in predictive modelling**

Basic assumptions	Conceptual model and its geometrical representation	Input parameters	Calibrated parameter	Predicted parameter	Model size	Discretisation	Numerical solution
The flow is assumed to be steady state and is determined by the transmissivity field and boundary conditions.	The flow domain is a series of 2D planar fractures with spatially variable aperture. The statistical parameters for each fracture may be different.	Statistics of random aperture fields (mean and covariance).	Mean aperture	Drawdown in the borehole sections	50m × 20m	The flow domain is discretized into $n_x \times n_y$ elements. Each element has the dimension $dx \times dy \times 2b$ , $b$ is half-aperture of the element.	The governing flow equation is solved using the code MODFLOW, using the finite difference method.

**Table 1-5 POSIVA - Breakdown of flow model used in predictive modelling**

Basic assumptions	Conceptual model and its geometrical representation	Input parameters	Calibrated parameters	Predicted parameters and entries	Model size	Discretisation	Numerical solution
It is sufficient to examine only the streamtube connecting the source and sink of the tracer test.	Properties of the streamtube are examined using the Discrete Fracture Network (DFN) approach. Fractures are assumed to have variable aperture.	An isotropic spatial model of the variability. Fracture geometry of the main fractures.	No need for calibration, only variability studied with this model.	Distribution of the flow rate along the flow channel (WL/Q).  Length of the flow channel.	The model contains the main fractures of the flow path. The modelling domain may be represented by a 2D chain of fractures with accordingly changing fracture properties. Size of the domain represented in the model will be few tens of metres by each side.	As fine discretisation as possible will be used taking into account the spatial model and the size of the modelling domain.	Finite element method using direct or iterative solver.

**Table 2-1 ENRESA - Breakdown of transport model used in predictive modelling**

Basic assumptions	Conceptual model and its geometrical representation	Input parameters	Calibrated parameters	Predicted parameters and entities	Model size, discretisation (coupling flow-transport)	Numerical solution
Background important, heterogeneity in back-ground and fracture planes. Matrix diffusion assumed active process.	Smaller domain considered with finer discretisation in some parts of the domain (where higher concentration gradients are expected). Fracture planes represented as 2D embedded features in the 3D rock mass.	$K(x,y,z)$ , boundary conditions from flow model. Initial concentrations, dispersivities, porosity, retardation coefficient, molecular diffusion coefficient.	$K$ , porosity, dispersivity, retardation.	$C(x,y,z,t)$	$K$ and bcs from flow. Smaller domain. Element sizes have a large variability (they can range from 1 m side in very close areas to the tracer test, and 20 m side near the contour of the model). Therefore scaling of $K$ values from flow model is needed.	Numerical; finite elements in space and implicit finite differences in time.

**Table 2-2 NIREX/AEAT - Breakdown of transport model used in predictive modelling**

Basic assumptions	Conceptual model and its geometrical representation	Input parameters (spatial model)	Calibration/prediction	Discretisation	Numerical solution
<p>The basic assumption is that groundwater flow and transport take place along fracture planes.</p>	<p>The basic conceptual model is that flow takes place in a Discrete Fracture Network (DFN) in which the heterogeneity is represented as variable aperture fractures. A set of background fractures will be included to account for the 'other' conductive features in the borehole.</p>	<p>Transport calculations will be performed using the rock-matrix diffusion algorithm in NAPSAC. This includes the processes of <i>rock-matrix diffusion</i> and <i>sorption</i>. Key parameters derived from laboratory estimates for <math>K_d</math> etc., with uncertainty (this would be the baseline estimates).</p>	<p>Before prediction of the sorbing tracer test, a calibrated flow model will be constructed. This calibrated model will use the relevant pre-test results, the Phase A and Phase B results (breakthrough) for predictions of:  Dilution (not already calibrated); Breakthrough characteristics. The calculations would account for the uncertainty in the input parameters.</p>	<p>The discretisation is the same as of the flow model.</p>	<p>Using a Laplace transform algorithm.</p>

**Table 2-3 JNC/Golder - Breakdown of transport model used in predictive modelling**

Basic assumptions	Conceptual model and its geometrical representation	Input parameters (transport model)	Model size	Discretisation	Numerical solution
<p>The basic assumption is that transport in fracture networks is controlled by processes of advection, dispersion, diffusion, and sorption.</p>	<p>The overall conceptual model is the same as in the flow model. For transport, each pipe within the network is assumed to consist of an advective connection, with one or more connected immobile zones. Diffusion occurs between mobile and immobile zones, and sorption occurs within immobile zones and on the surface area of the advective pipes.</p>	<p>The input required for transport simulations include dispersion, diffusion, and sorption parameters; definition of immobile zones; and correlations between flow parameters and transport properties such as transport aperture and transport width.</p>	<p>The domain sizes of the flow and the transport models are the same.</p>	<p>The discretisation is the same as that of the flow model.</p>	<p>Transport is solved by the Laplace Transform Galerkin method.</p>

**Table 2-4 SKB/LaSAR - Breakdown of transport model used in predictive modelling**

Basic assumptions	Conceptual model and its geometrical representation	Input parameters	Calibrated parameter	Predicted parameters	Model size	Discretisation	Numerical solution
All mass transfer processes are linear. The sorption on the inner surfaces of the rock matrix and on fracture surfaces are assumed to be at equilibrium. The sorption in gouge material is assumed to be first-order kinetically reversible. $\theta$ and $D$ are constants.	The tracer is transported advectively in the fracture, is dispersed due to velocity variation and is subject to various mass transfer processes (Diffusion/sorption in the rock matrix, sorption on fracture surfaces and sorption in gouge material); 1D diffusion in matrix.	Advective velocity field ; diffusion and sorption parameters; Input (injection) function.	The parameter $B$ for diffusion/sorption in the rock matrix. The parameters for sorption in gouge material.	Breakthrough curve for each tracer and each test including $t_5$ , $t_{50}$ , $t_{95}$ , mass recovery;	50m × 20m	The same as in flow model	The particle tracking technique with Monte-Carlo simulation is used to obtain $\beta$ - $\tau$ distribution (or relationship). Analytical/integral expressions for the BTC are available; numerical quadrature done by the trapezoidal method.

**Table 2-5 POSIVA - Breakdown of transport model used in predictive modelling**

Basic assumptions	Conceptual model and its geometrical representation	Input parameters	Calibrated parameters	Predicted parameters and entities	Model size	Discretisation	Numerical solution
Transport takes place along a streamtube (channel).	Transport in channel/-s is having a linear velocity profile. Molecular diffusion in the channel and into the rock matrix and stagnant areas are taken into account.	Flow rate through the transport channel(s), geometric dimension of the channel(s), rock matrix properties, sorption, volume aperture.	If suitable tracer tests exist: Volume aperture, field scale sorption coefficient, distribution of the flow rate (WL/Q).	Spreading in the breakthrough curve. Breakthrough curve for delta function input and for the measured source term.	Not applicable Analytical model.	Not applicable Analytical model	Analytical solution for the advection-dispersion coupled with analytical matrix diffusion model.



# Appendices



## **NIREX/AEAT approach and code summary**



## A2.1 Introduction

AEA Technology will carry out discrete fracture network groundwater flow and transport modelling using NAPSAC. The objective of the modelling work to be performed for the TRUE Block Experiment is to represent heterogeneity on the fracture plane that reflects the heterogeneity observed from hydraulic and dilution tests using appropriate geostatistical models. At this point we are not making any phenomenological assumptions regarding the structure of flow channels.

Groundwater flow in many hard rocks is believed to occur within discrete fractures. Radionuclides in solution can diffuse away from the fractures into immobile water in the rock matrix. This process (rock-matrix diffusion) is important in determining the performance of a repository situated in fractured rock because it retards the transport of radionuclides that might otherwise return rapidly to the biosphere. Therefore rock-matrix diffusion has been explicitly represented in the models of radionuclide transport that have been used in probabilistic system assessment (PSA) calculations for deep repositories. However, the models of rock-matrix diffusion used in PSA calculations have to be simple, and various approximations have to be made. For example, in the model used in assessment studies the fractures are often arranged regularly and have the same properties, whereas in a real fracture network the fractures are arranged irregularly and their properties (such as aperture) vary from fracture to fracture and within a single fracture.

Direct applicability of this simple model is limited by several complicating factors. First, there may be geometric complexities in the fracture system, with multiple intersecting fracture sets, so that the average water flow direction may not lie parallel to any set of fracture planes. Secondly, flow in the fractures may be principally along channels that occupy a small fraction of the area of each fracture plane. This reduces the area for transfers between the fractures and the matrix, and changes the geometry for the diffusion process, allowing the radionuclides to spread out over greater areas as they proceed into the matrix. In order to address these complexities of rock-matrix diffusion in real fracture systems, it is desirable to include an explicit representation of rock-matrix diffusion in fracture network models.

NAPSAC is a computer program used to model groundwater flow and transport in fractured rock. The models are based on a direct representation of the discrete fractures making up the flow-conducting network. A stochastic approach is used to generate networks of planes with the same statistical properties as those measured for fractures in field experiments. A very efficient finite-element method is used to solve the equations for flow in a network. The transport option is designed to calculate the migration and dispersal of a tracer through a network for which the flow has been determined. The algorithm is based on particle tracking.

This summary describes the basic mathematics of NAPSAC and the sorption and rock-matrix diffusion model in NAPSAC relevant to the TRUE Block Scale Project. A fuller description illustrating its full functionality may be found in Hartley (1998).

AEA Technology developed the NAPSAC fracture-network modelling software to simulate flow, tracer and mass transport through fractured rock.

## **A2.2 The Discrete Fracture Network Approach**

In the DFN approach, the geometry of the fracture-network is accounted for explicitly. The approach is needed to describe or predict aspects of the performance of the fractured system where the geometry of the fracture-network plays a significant role.

Some examples of such circumstances are:

- representations of any flow experiments where the fracture connectivity is important, which in practice means almost all interpretations of field experiments where a detailed understanding is needed;
- prediction of the effective flow properties of the fracture-network system and of the scale dependence of effective properties;
- prediction of the effect of the fracture-network geometry on the effective dispersion for solute transport;
- prediction of the effect of the fracture-network geometry on the effective hydraulic diffusivity of the pressure field in response to a pressure change and the inferred radius of influence of pressure tests.

From the above list, it can be seen that an understanding of the role of the fracture geometry can be important in almost all aspects of an investigation of a fractured rock system. The two main reasons that such discrete models are not more commonly used are the complexity of the models and the fact that stochastic models inevitably require uncertainty to be addressed formally.

The complexity means that a large quantity of data is required to characterise fracture systems adequately. Whilst there are still issues to be resolved in the experimental characterisation of fracture-network flow geometry, a number of research projects for the radioactive waste industry such as the TRUE Block Scale Experiment have demonstrated the possibility of collecting suitable basic input data.

Understanding fracture channelling and the extent of the flow wetted surface (or WL/q as described by POSIVA) of the fracture are still research tasks, but simple assumptions can be made and the other data interpreted consistently so that the resulting fracture-network geometry reproduces key features of the physical network. In many cases however there will be a balance between the benefits of a more detailed representation of the system, and the increased cost of collecting data for which there may be significant uncertainty.

The second reason why the discrete fracture-network approach is not more widely used is the need to treat predictions in a probabilistic framework and consider the uncertainty due to the details of the fracture geometry directly.

Applications of NAPSAC particular to the TRUE Block include:

- modelling of flow and transport in regional fracture-network systems, including the effects of salinity;
- providing a local scale fracture network ‘structural’ groundwater flow and transport model, including the heterogeneity on the fracture planes.

The list of NAPSAC (Release 4.2) capabilities includes:

- simulation of steady-state or transient fluid flow in a fracture-network. Steady-state calculations use an efficient finite-element scheme to enable calculations on very large networks. Transient calculations use domain decomposition to give good accuracy where changes take place rapidly without introducing high run times for the rest of the network;
- calculation of the full effective permeability tensor including off-diagonals, principal values and directions. This is automated to sample flows in many different directions. This can be used for up scaling, analysis of scale dependencies and determination of the representative elementary volume (REV);
- prediction of transient pressures and drawdowns at well bores for various types of pump tests;
- calculation of steady-state and transient inflows to tunnels and shafts;
- calculation of the effects of hydro-mechanical coupling. The hydraulic aperture is coupled to a stress distribution based on an analytical description of the stress field due to either rock weight or a radial stress around a tunnel;
- simulation of tracer transport through the network using a stochastic particle tracking method. Output includes plots of breakthrough curves for many thousands of particles, particle tracks, swarms of particles at specified times or the points of arrival on the surfaces of the model. This can be used to calculate dispersion of a solute transported by the groundwater;
- simulation of mass transport for a variable density fluid. This can be used to model coupled groundwater flow and salt transport;
- generation of stochastic fractures from a wide variety of probability distribution functions;
- inclusion of deterministic fractures by specification within the NAPSAC data or by importing a fracture file;
- analysis of percolation between surfaces;
- examination of the network using hypothetical cores, stereonets and fracture maps;
- 3D visualisation of results using the AVIZIER for NAPSAC software.

## A2.3 NAPSAC calculations

This Section briefly describes the mathematics behind the groundwater flow and transport calculations relevant to the TRUE Block modelling. A fuller description can be found in Hartley (1998).

### Steady-State Flow

The groundwater flow is assumed to occur entirely within the fracture-network, and the groundwater is assumed to be incompressible so that mass conservation implies

$$\nabla \cdot \mathbf{q} = 0 \quad (\text{A2-1})$$

where  $\mathbf{q}$  is the groundwater volume flux. The pressure at each global flow node is calculated by solving equations (A2-1) and (A2-3) subject to the prescribed boundary conditions. Note: NAPSAC works in terms of the dynamic pressure,  $P$  which is related to the total pressure,  $P_T$ , by  $P = P_T - \rho g h$  where  $\rho$  is fluid density and  $z$  is the vertical height relative to some datum. The finite-element approach is used. The weak form of the problem is obtained by multiplying equation (1-1) by a suitable test function and then integrating over the flow domain,  $\Omega$ . The pressure field is approximated by a function of the pressure values at the global nodes,  $P_I$ , with piecewise linear basis functions defined along each intersection. These basis functions are defined over the fracture planes, away from the intersections in the following way.

Noting that the groundwater flux is linearly dependent on the gradient of the pressure, and using the Galerkin finite-element formulation, the problem of solving the mass conservation equation becomes one of solving

$$\sum_J \hat{T} \int_{\Omega} \Psi_I \nabla^2 \Psi_J P_J = 0, \quad (\text{A2-2})$$

for suitable basis functions  $\Psi_I$  where  $T_I$  is a constant related to the transmissivity  $T$  by  $T = \rho g T$ . Here  $\rho$  is the fluid density and  $g$  is acceleration due to gravity. Defining

$$F_{IJ} = \hat{T} \int_{\Omega} \Psi_I \nabla^2 \Psi_J P_J, \quad (\text{A2-3})$$

so that  $F_{IJ}$  is the net flux due to unit pressure at node  $J$  and zero pressure at all other global flow nodes, integrated over the basis function for node  $I$  along the intersection containing node  $I$  (mass conservation on the fracture plane requires that  $\nabla^2 \Psi_J$  is zero elsewhere in the solution domain). Both the fractures that include the intersection containing global flow node  $I$  will make a contribution,  $f_{IJ}^{(k)}$ , to  $F_{IJ}$ .

The next stage of the NAPSAC groundwater flow calculation is to evaluate  $f_{IJ}^{(k)}$  for each fracture plane  $k$  and each pair of global flow nodes  $I, J$ . The finite-element method is used to solve the mass conservation equation (1-1) on the fracture plane. Assuming laminar viscous flow between two parallel plates with a separation equal to the fracture aperture, the groundwater volume flux  $\mathbf{q}$  over the surface of the fracture plane is



$$\mathbf{q} = \frac{e^3}{12\mu} \nabla P \quad (\text{A2-4})$$

where  $e$  is the fracture aperture and  $\mu$  is the viscosity of the groundwater. The transmissivity of the fracture plane is given by

$$T = \frac{\rho g e^3}{12\mu} \quad (\text{A2-5})$$

the parallel-plate law of transmissivity.

Each fracture plane is discretised into a user-specified number of linear triangular finite-elements. The line of a fracture intersection is approximated so as to coincide with the edges of the triangular elements generated by the fracture discretisation.

The final stage of the groundwater flow calculation is to evaluate the pressure field in the fracture-network. The matrix equation (A2-2) is assembled. The global boundary conditions are imposed, and a direct frontal solver is used to calculate the pressure values at the global flow nodes from the matrix equation. The pressure distribution across a fracture plane can be recovered by the superposition of the individual basis functions calculated earlier, weighted by the pressure solution at the global flow nodes.

## A2.4 Tracer transport

The tracer transport option in NAPSAC is designed to calculate the migration and dispersal of tracer through a discrete fracture-network. Within the groundwater, it is assumed that tracer transport is dominated by advection, so that molecular diffusion can be ignored, and the major cause of dispersion is due to the existence of a number of different paths through the fracture network. It is also assumed that the fracture apertures are small enough that the tracer diffuses quickly across the aperture.

The transport calculations are based upon a particle-tracking algorithm. The problem is split up into the calculation of single fracture responses followed by the calculation of the transport of a particle swarm through the network. For each fracture plane a representative number of pathlines between the intersections on the plane are calculated. Intersections are discretised by transport nodes and pathlines are calculated from each transport node. There are two algorithms available for calculating these pathlines.

The first algorithm provides 'exact particle tracking'. For each fracture, the flow field is discretised in terms of linear triangular finite-elements. The flow is determined by the pressure field, and since the pressure varies linearly over each triangle, the groundwater velocity,

$$v = \frac{\mathbf{q}}{e} = \frac{e^2}{12\mu} \nabla P \quad (\text{A2-6})$$

is constant on each element. The pathlines are calculated on each fracture by stepping the path across the mesh, one element at a time. On reaching a fracture intersection, the path is complete. Once the pathlines from the transport nodes on each fracture plane have been calculated, the possible connections for that node are determined. A list of

possible destinations, travel times, distances and relative probabilities for a particle leaving each node are calculated. In this way, a library of paths is created for every transport node in the network. The model relies on the calculation of a very accurate flow solution. If a low accuracy solution is used, then problems with local flow sinks on fractures may occur, resulting in the loss of a significant fraction of the particle swarm.

## A2.5 The Rock-Matrix Diffusion and Sorption Model

Typically simple models of rock-matrix diffusion are used in PSA calculations. The model corresponds to flow in infinite parallel fractures with constant aperture and spacing, with diffusion into the matrix between the fractures. The flow and distribution of concentration for each symmetry unit around a fracture are taken to be the same for all the symmetry units. A one-dimensional model of diffusion normal to the fractures is used, neglecting diffusion parallel to the fracture. This model is perhaps the simplest model of rock-matrix diffusion.

The equations that characterise the model are as follows. The equation for radionuclide transport in a fracture is

$$R \frac{\partial c}{\partial t} = -v \frac{\partial c}{\partial x} + D_l \frac{\partial^2 c}{\partial x^2} + \frac{2D_i}{b} \frac{\partial c^P}{\partial w} (w = 0), \quad (\text{A2-7})$$

where

$R$  is a retardation factor due to linear equilibrium sorption on the fracture walls;

$c(x, t)$  is the concentration of radionuclide in the fracture pore water;

$v$  is the transport velocity of water in the fracture;

$D_l$  is the longitudinal dispersion coefficient;

$D_i$  is the intrinsic diffusion coefficient within the rock matrix;

$b$  is the fracture aperture;

$c^P(x, w, t)$  is the concentration of radionuclide in the rock matrix porewater;

$x$  is the coordinate along the fracture;

$w$  is the coordinate perpendicular to the fracture;

$t$  is time.

The equation for the diffusion of radionuclide into the rock matrix is

$$\alpha \frac{\partial c^P}{\partial t} = D_i \frac{\partial^2 c^P}{\partial w^2}, \quad (\text{A2-8})$$

where

$\alpha$  is the capacity factor of the rock matrix.

The above equations are supplemented by the initial conditions

$$c(x,0) = 0 \quad (\text{A2-9})$$

$$c^P(x,w,0) = 0 \quad (\text{A2-10})$$

and the boundary conditions

$$c(0,t) = I(t) \quad (\text{A2-11})$$

$$c^P(x,0,t) = c(x,t) \quad (\text{A2-12})$$

$$\frac{\partial c^P}{\partial w}(w=d) = 0, \quad (\text{A2-13})$$

where

$I(t)$  is the concentration of radionuclide at the ‘inlet’;  
 $d$  is the distance that the radionuclide can diffuse into the rock matrix,  
which is half the spacing of the fractures.

These equations can be solved by the method of Laplace transforms. For example, if the equations are simplified by taking:

$R = 1$ , that is the radionuclide is non-sorbing, or  $K_d = 0$ ;  
 $D_l = 0$ , that is there is no longitudinal dispersion;

then the Laplace transform,  $\bar{c}$ , of  $c$  is given by

$$\bar{c}(x,s) = A(s)e^{-\frac{g(s)}{v}x}, \quad (\text{A2-14})$$

where

$$g(s) = s + \frac{2D_i}{b}\psi \tanh(\psi a) \quad (\text{A2-15})$$

$$\psi = \sqrt{\frac{\alpha s}{D_i}} \quad (\text{A2-16})$$

and  $A(s)$  is determined from the boundary condition

$$A(s) = \bar{I}(s). \quad (\text{A2-17})$$

$\bar{I}(s)$  is the Laplace transform of  $I(t)$ . This expression can be inverted numerically using, for example, Talbot’s algorithm [Reference] to determine

$$c(x,t). \quad (\text{A2-18})$$

The above analysis can be used as the basis of analysis for more complicated cases. For example, considering flow and transport along a fracture comprising several sections with different properties then

$$\bar{c}_i(x,s) = A_i(s) e^{-\frac{g_i(s)}{v_i} x} \quad \text{for } x \text{ in section } j, \quad (\text{A2.19})$$

where the subscript  $i$  identifies the section, and  $A_i$  is determined by continuity between the sections.

## A2.6 The Transport Algorithm

The transport option in NAPSAC is designed to calculate the migration and dispersal of a tracer through a fracture network for which the flow solution has been determined. The transport of a tracer is modelled by tracking a swarm of particles. In order to simulate transport through large networks, each particle track is broken down into its component paths which connect intersections on fracture planes. A particle is followed by selecting appropriate steps from this ‘connection library’. Two approaches to calculating the ‘connection library’ are available:

- (a) if a highly discretised flow solution is obtainable, direct pathline calculations can be performed (exact particle tracking);
- (b) if the discretisation is coarse (eg. because the network is large), a robust ‘equivalent flux connection’ which avoids the loss of particles to numerical sinks on the fracture planes can be determined (approximate particle tracking).

### *Exact particle tracking*

For each fracture, the flow field is discretised in terms of linear triangular finite-elements arranged in blocks of four triangles to give a rectangular mesh. The flow is determined by the pressure field, and since the pressure varies linearly over each triangle, the groundwater velocity is constant on each element.

A representative number of pathlines are calculated on each fracture by stepping the path across the mesh one element at a time. For each element, the intersection of the path with the element boundaries is calculated, and the path leaves the element at the first of these intersections. The element into which the path has crossed is considered next, and a check is made to determine whether the path has reached a fracture intersection. On reaching a fracture intersection the path is complete.

There are several numerical problems associated with this method, and the ‘exact particle tracking’ algorithm is controlled by a set of accuracy parameters that can be adjusted to minimise the number of ‘lost’ particles. In particular, each path is associated with a weight function at an intersection, and the paths are started from the centre of these weight functions.

Once the pathlines from the transport nodes on each fracture plane have been calculated, the possible connections for that node are determined. A list of possible destinations, travel times, distances and relative probabilities for a particle leaving each node are calculated. In this way, a library of paths is created for every transport node in the network.

The model relies on the calculation of very accurate flow solutions. If a low accuracy solution is used, then problems with local flow sinks on fractures may occur, resulting in the loss of a significant fraction of the particle swarm.

### *Approximate particle tracking*

NAPSAC is able to create a database that records the net flux between all the intersections for a flow solution. This network of flux connections links the centre of every intersection on a given fracture to every other intersection centre on the fracture. The flow from intersection centre to intersection centre is calculated as

$$Q^{ij} = \sum_{k,l} f_{lk}^{ji} P_k^i - \sum_{l,k} f_{kl}^{ij} P_l^j \quad (\text{A2-20})$$

where  $P_k^i$  is the head at node  $k$  of intersection  $i$ , and  $f_{kl}^{ij}$  is the flow induced at node  $k$  of intersection  $i$  by a unit pressure at node  $l$  of intersection  $j$ . A transport option has been developed that is based on this flux database.

One of the main difficulties with the ‘equivalent flux connection’ approach to particle transport is how to associate a distance and a travel time to each connection. If we assume ‘plug’ flow in the connections, then the problem of assigning a travel time to the flow in a connection is that of assigning an effective area to the connection (since we know the aperture of the plane containing the connection). A model of the effective area is

$$a^{ij} = g^{ij} \frac{A}{\sum_{Q^y > 0} \frac{g^{ij}}{Q^y}} \quad (\text{A2-21})$$

where  $g^{ij}$ , the geometric area associated with intersections  $i$  and  $j$ , is weighted by the inverse of the flux  $Q^y$  and scaled so that the total area equals the fracture area  $A$ .

The pathlines calculated by the exact particle tracking method may be tortuous; the ‘equivalent flux connection’ model can’t represent this dispersion on a single plane accurately. However, if dispersion is dominated by the different paths through a fracture network rather than by dispersion on a single plane, then this inaccuracy may be small. The ‘equivalent flux connection’ model is therefore expected to perform most accurately for large networks, where the exact particle tracking method would be prohibitively expensive.

A second inaccuracy arises from the mixing that is assumed to occur at each fracture intersection, which is a consequence of the single connection between each pair of intersections. This implies that the ‘equivalent flux connection’ model will tend to underestimate the dispersion in a fracture network.

## A2.7 Diffusion coefficients

The migration of a chemical species under a composition gradient is characterised by a material dependent parameter known as the diffusion coefficient. This coefficient is defined by

$$\frac{\partial c}{\partial t} = \frac{\partial}{\partial x} D \frac{\partial c}{\partial x} \quad (\text{A2-22})$$

where  $c$  is the concentration and  $D$  is the diffusion coefficient. For one-dimensional diffusion in an isotropic medium with a constant diffusion coefficient this equation reduces to Fick’s laws of diffusion.

There can be confusion over the definitions of the various diffusion coefficients, and so they are briefly discussed here. The diffusive flow of a species under a concentration gradient that is constant with respect to both time and position is described by Fick’s first law of diffusion

$$J = -D_m \frac{\partial c}{\partial x} \quad (\text{A2-23})$$

where  $J$  is the molecular flow-rate (flux density). For diffusion in a porous medium, it is often more convenient experimentally to monitor the average flow-rate per unit area of the porous medium (denoted  $\langle J \rangle$ ) and to control the concentration in the aqueous phase. In this case, Fick’s law becomes

$$\langle J \rangle = -D_i \frac{\partial c}{\partial x} \quad (\text{A2-24})$$

$D_i$  is the intrinsic diffusion coefficient, and is considered to be mainly a characteristic of the medium. It is also possible to define an average concentration in the porous medium as a whole (denoted  $\langle c \rangle$ ). Use of this definition of concentration leads to a further equation

$$\langle J \rangle = -D_{\text{eff}} \frac{\partial \langle c \rangle}{\partial x} \quad (\text{A2-25})$$

$D_{\text{eff}}$  is the apparent diffusion coefficient, and is related to the intrinsic diffusion coefficient by

$$D_{\text{eff}} = \frac{D_i}{\alpha} \quad (\text{A2-26})$$

where  $\alpha$  is the capacity factor.

### *The Rock-Matrix Diffusion Algorithm*

The effect of rock-matrix diffusion is to increase the travel times of particles being transported through a fracture system. Two algorithms for calculating the increase in travel times were considered.

#### *Particle tracking algorithm*

A diffusion process can be described in terms of:

- (a) either a diffusion equation

$$\frac{\partial c}{\partial t} = \frac{\partial}{\partial x} D \frac{\partial c}{\partial x} \quad (\text{A2-27})$$

where  $c$  is the concentration and  $D$  is the diffusion coefficient;

- (b) or equivalently a stochastic differential equation of motion for the individual particles

$$\frac{dx}{dt} = \sqrt{2D} \eta(t) \quad (\text{A2-28})$$

where  $\eta(t)$  is a Gaussian random variable

$$\langle \eta(t) \rangle = 0 \quad (\text{A2-29})$$

$$\langle \eta(t)\eta(t') \rangle = \delta(t - t'). \quad (\text{A2-30})$$

The transport equations in NAPSAC can be modified using (A2-28) in order to model a diffusion process. In particular, the rock-matrix diffusion equations (A2-7) and (A2-8) imply that for each particle:

- (a) If  $\left(-\frac{b}{2} < w < \frac{b}{2}\right)$ , so that the particle is located in the fracture,

$$\frac{dx}{dt} = v \quad (\text{A2-31})$$

$$\frac{dw}{dt} = \sqrt{2D_m} \eta(t). \quad (\text{A2-32})$$

- (b) The probability of a particle crossing from the fracture into the rock matrix is  $D_i/D_m$ .

(c) If  $\left(w < -\frac{b}{2}\right)$  or  $\left(\frac{b}{2} < w\right)$ , so that the particle is located in the rock matrix,

$$\frac{dx}{dt} = 0 \quad (\text{A2-33})$$

$$\frac{dw}{dt} = \sqrt{2\frac{D_i}{\alpha}} \eta(t). \quad (\text{A2-34})$$

(d) The boundaries at  $(w = -a)$  and  $(w = a)$  are reflecting boundaries.

However, algorithms based on the above equations require an excessive amount of computer time. The reason for this is that a typical fracture aperture is  $b = 10^{-6}$  m and a typical intrinsic diffusion coefficient is  $D_i = 10^{-7}$  m<sup>2</sup>/year, and so the ‘return’ time that a particle spends in the fracture before re-entering the rock matrix is

$$\frac{\text{time to diffuse a distance equal to the fracture aperture}}{\text{probability to cross from the fracture into the rock matrix}} = \frac{b^2 D_m}{2D_m D_i} \quad (\text{A2-35})$$

$$\approx 5 \times 10^{-6} \text{ year}$$

Since a typical travel time along a fracture is of the order of a year, each particle will undergo about  $2 \times 10^5$  ‘random walks’ in the rock matrix while crossing the fracture. This is an unreasonably large number, and therefore this algorithm is not acceptable.

### *Laplace transform algorithm*

An alternative algorithm assumes that the aperture of fracture  $i$  in the fracture network is uniform, in which case the Laplace transform of the cumulative probability distribution of particle travel times between two transport nodes on the fracture can be deduced from equation (A2-19)

$$\bar{p}(s) = \frac{1}{s} e^{-\text{TIMOUT} g_i(s)} \quad (\text{A2-36})$$

Here the NAPSAC variable TIMOUT is the integrated travel time on the fracture given by

$$\text{TIMOUT} = \int \frac{dx}{v}. \quad (\text{A2-37})$$

This expression can be inverted using Talbot’s algorithm [Reference] to calculate

$$p(t) \quad (\text{A2-38})$$

A travel time on the fracture, taking into account rock-matrix diffusion, can be calculated for each particle from this probability distribution.



## **JNC/Golder approach and code summary**



## A3.1 Flow modeling in FracMan/PAWorks

JNC/Golder are carrying out steady state and transient flow modelling for the TRUE-Block scale project using a single porosity, constant fluid density channel network approach (CN). Solutions are obtained using FracMan/PAWorks software

### A3.1.1 Basic assumptions

The FracMan/PAWorks model assumes that flow occurs exclusively in discrete features, and that these features can be approximated as 3D networks of rectangular cross-section pipes. FracMan/PAWorks assumes laminar (Darcy) flow according to the equation (Bear, 1972),

$$S \frac{\partial h}{\partial t} - T \frac{\partial^2 h}{\partial x^2} = q \quad (\text{A3-1})$$

Where the fundamental properties of fractures for flow are the transmissivity  $T$  ( $\text{m}^2/\text{s}$ ), and storativity  $S$  (-). The transmissivity can be thought of as a confined aquifer hydraulic conductivity-thickness

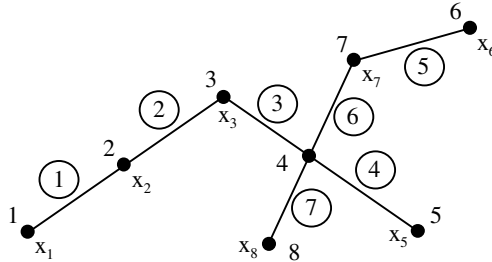
$$T = K e \quad (\text{A3-2})$$

where  $K$  is hydraulic conductivity ( $\text{m/s}$ ) and  $e$  is a “hydraulic” aperture ( $\text{m}$ ). However, in PAWorks, the fundamental equations are solved directly in terms of  $T$  and  $S$ , and it is therefore not necessary to rely on concepts of “hydraulic” aperture and “cubic law”. Porosity is included in the effective transmissivity and storativity values, and therefore does not need to be considered explicitly for flow solutions.

FracMan/PAWorks, as currently used in the TRUE Block Scale project, is a single porosity solution, in which all flow and hydraulic storage is provided by the pipe element channels. Dual permeability and dual porosity flow assumptions are available in FracMan/MAFIC software, but were not deemed necessary for the current modelling tasks. Variable density flow assumptions are available in FracMan/MAFIC but are also not utilized in the current modelling.

### A3.1.2 Geometric concepts

The channel network concept as implemented by JNC/Golder is an extension of the discrete fracture network (DFN) concept. Each fracture is treated as a discrete plane. The intersections between fractures define “traces” which are line elements. Channel elements are defined between each of the trace combinations, until the channel network is sufficient to provide connectivity between the traces comparable to that of the DFN



model. Pipes are defined between nodes at the centre of fracture traces. Where fracture intersections are considered to be potentially significant flow elements, the traces themselves are also modelled as pipes.

Pipe channels are described geometrically by the nodal coordinates of the pipe ends, and by the pipe width and length. Pipe transport aperture  $e$  is used for transport solutions, but is not considered for flow solutions

### A3.1.3 Input parameters

PAWorks channel network input parameters consist of the following

- Fracture network, a file containing the geometry and properties of each of the fractures to be modelled in the fracture network. For each fracture in the fracture network, this includes the nodes at the corner of the fracture, the fracture transmissivity, storativity, and transport aperture.
- Pipe topology assumption, which selects the algorithm used to transform the fracture network to a channel network. This ranges from a minimal solution of the minimum set of channels necessary to obtain the connectivity of the DFN to a network with sufficient channels to ensure that the tortuosity of the channel network is not greater than that of streamlines in the DFN. This also includes the choice as to whether to include fracture intersections as flowing elements in the model.
- Channel width assumption, which determines how channel widths are assigned. This ranges from simple averaging of the lengths of traces to complex model assumptions which provide for channelization area percentages on fracture planes.

#### **A3.1.4 Spatial model**

The spatial model used by JNC/Golder combines planar discrete features representing all the numbered discrete structures in the TRUE Block Scale rock volume. In addition, the model include stochastic and conditioned discrete features based on analysis of Posiva flow logs, BIPS logs, and hydraulic testing.

Several alternative assumptions will be made concerning the spatial structure of flow channels. These will include approaches which include fracture intersection traces as flow elements, models which ignore fracture intersection traces, and models which consider only traces formed by intersections of major discrete features.

#### **A3.1.5 Model scale**

The TRUE Block Scale model is being implemented as a nested model within the 500 m scale to meet the boundary conditions established by the project. Numbered structures are modelled to the full 500 m scale. However, background fracturing is only modelled on a scale of 50 to 100 m directly around the discrete features of interest. In addition, detailed modelling of channel structure will only be provided in the direct vicinity of Structures #13, #20, #21, and #22.

#### **A3.1.6 Discretization**

The “pipe” is the finest flow element included in the PAWorks model. Pipes are discretized to a scale of approximately 5 m (the average distance between fracture intersections). Approximately 150,000 pipes are used for the solution.

#### **A3.1.7 Numerical solution**

The flow field is solved by applying the Galerkin method to the governing equation (Equation A3-1):

$$\int_L \left( S \frac{\partial \hat{h}}{\partial t} - T \frac{\partial^2 \hat{h}}{\partial x^2} - q \right) \xi_n dx = 0, n = 1, 2, \dots, N. \quad (\text{A3-3})$$

where,

- $\hat{h}$  = the approximate solution of head,
- N = total number of nodes,
- L = length of the domain.

## A3.2 PAWorks Transport models

JNC/Golder are carrying out transport model within PAWorks channel network (CN) model using Laplace Transform Galerkin solution for transport equations. Solutions are obtained using FracMan/PAWorks software.

### A3.2.1 Basic assumptions

Transport is solved assuming steady-state flow and a second-order approach to describe the diffusive mass transfer of a solute between the groundwater in a pipe and the multiple immobile porosity zones attached. The solution assumes:

- advective transport in pipe network
- longitudinal dispersion within pipes
- complete mixing at pipe intersections
- diffusive exchange with immobile zones connected to each pipe
- sorption to pipe walls and within immobile zones
- decay of solute species

### A3.2.2 Conceptual model

The advective-dispersive, diffusive transport of solute species  $n$  in a pipe network is given by:

$$A \left[ R_n(\lambda) \frac{\partial C_n}{\partial t} + q(\lambda) \frac{\partial C_n}{\partial \lambda} - \frac{\partial}{\partial \lambda} D_{\lambda_n}(\lambda) \frac{\partial C_n}{\partial \lambda} + R_n(\lambda) \lambda_n C_n - R_{n-1}(\lambda) \lambda_{n-1} C_{n-1} \right] \pm \sum_{\lambda^*} \dot{M} \delta(\lambda - \lambda^*) + \sum_{\lambda^*} Q(C_n - C_n^*) \delta(\lambda - \lambda^*) + \sum_{im=1}^M V_{im} \theta_{im} D_{im} \frac{\partial C_n^{im}}{\partial w} \Big|_{w=0} = 0 \quad (\text{A3-4})$$

where:

- $n$  = trace index [-]  
 $im$  = immobile zone class number (note: if desired  $im$  can equal 0) [-]  
 $IM(\lambda)$  = total number of immobile zones attached to pipe  $\lambda$  [-]  
 $A(\lambda)$  = pipe cross-sectional area [ $L^2$ ]  
 $R_n(\lambda)$  = retardation factor [-]  
 $q(\lambda)$  = specific discharge ( $\equiv$  Pipe velocity  $v$ ) [ $L/T$ ]  
 $D_{\lambda_n}(\lambda)$  = dispersion coefficient =  $\alpha v + D_n^o$  [ $L^2/T$ ]  
 $\alpha$  = pipe longitudinal dispersivity [ $L$ ],  
 $D_n^o$  = free-solution diffusion coefficient [ $L^2/T$ ]  
 $\lambda_n$  = decay constant [ $1/T$ ]

$\dot{M}(t)$	=	internal solute mass source/sink [M/T]
$Q$	=	external fluid source/sink [L <sup>3</sup> /T]
$\delta(\lambda - \lambda')$	=	Dirac delta [1/L]
$\delta(\lambda - \lambda^*)$	=	Dirac delta [1/L]
$V_{im}$	=	block surface area per unit volume of matrix and fissures [1/L]
$D_{im}$	=	matrix effective diffusion coefficient [L <sup>2</sup> /T]
$\theta_{im}$	=	immobile zone porosity for immobile zone “im”
$C_n$	=	pipe concentration [M/L <sup>3</sup> ]
$C_n^*$	=	concentration of injectate in external fluid source [M/L <sup>3</sup> ]
$C_n^{im}$	=	Immobile zone concentration [M/L <sup>3</sup> ]
$\lambda$	=	Distance along interconnected pipe network [L]
$\lambda'$	=	Location of solute mass source/sink [L]
$\lambda^*$	=	Location of external fluid source/sink [L]
$w$	=	Distance perpendicular to plane of fracture [L]
$t$	=	time [T]

It should be noted that if there is no flow along a particular pipe within the network (i.e.  $q(\lambda) = 0$ ), then the model allows for diffusive transport along the length of this pipe. It should also be pointed out that if fluid is withdrawn at a resident concentration  $C_n^* = C_n$ , then the term involving  $Q$  in (1) vanishes. If the injectate concentration  $C_n^* = 0.0$ , then this term accounts for the dilution effect of the injection of solute-free water.

The initial concentrations of all species within the domain are assumed to be zero in the current version of LTG. Boundary conditions may be either of the Dirichlet-type where the input concentration history of each species is a specified function of time, or of the Cauchy-type where the advective input mass flux can be prescribed as a function of time at the origin of a pipe on the boundary of the domain. Mathematically, these boundary conditions are described by:

$$\text{Dirichlet: } C_n = C_n^o(t) \text{ on } \Gamma \quad (\text{A3-5})$$

$$\text{Cauchy: } A(\lambda)q(\lambda)C_n^o(t) = A(\lambda) \left[ q(\lambda)C_n(\lambda, t) - D_{\lambda_n}(\lambda) \frac{\partial C_n}{\partial \lambda} \right] \text{ on } \Gamma \quad (\text{A3-6})$$

where  $C_n^o(t)$  is the specified concentration for species n. LTG also allows the concentration or flux rate (e.g. mol/yr) to be specified at an interior point.

### A3.2.3 Immobile zone

In order to represent the diffusive exchange of solute mass between the pipes and any on the *im* immobile zones attached to them, LTG uses a second-order approach described by:

$$\theta_{im}(im, \lambda) R_n^{im}(im, \lambda) \frac{\partial C_n^{im}}{\partial t} - \frac{\partial}{\partial w} \theta_{im}(im, \lambda) D_{im} \frac{\partial C_n^{im}}{\partial w} + \theta_{im}(im, \lambda) R_n^{im}(im, \lambda) \lambda_n C_n^{im} - \theta_{im}(im, \lambda) R_{n-1}^{im}(im, \lambda) \lambda_{n-1} C_{n-1}^{im} = 0 \quad (A3-7)$$

where:

$\theta_{im}(im, \lambda)$	=	Immobile zone porosity for immobile zone “ <i>im</i> ” attached to pipe “ $\lambda$ ” [-]
$R_n^{im}(im, \lambda)$	=	Immobile zone retardation factor for immobile zone “ <i>im</i> ” attached to pipe “ $\lambda$ ” [-]
$C_n^{im}$	=	Concentration in matrix [M/L <sup>3</sup> ]
$D_{im}$	=	Matrix effective diffusion coefficient [L <sup>2</sup> /T]
	=	$D_n^0 \tau$
$D_n^0$	=	Free-solution diffusion coefficient [L <sup>2</sup> /T]
$\tau$	=	Tortuosity [-]

If a particular immobile zone is fluid-filled, such as within an immobile water zone attached to a pipe within a fracture plane, then the immobile zone porosity,  $\theta_{im}$ , would equal 1.0.

The actual injection time history is directly solved at any desired location within the pipe network, in terms of both mass and concentration. Steady state flow is assumed.

### A3.2.4 Integration of flow and transport

JNC/Golder are using the same pipe networks for both flow and transport, such that flow and transport solutions are fully integrated.

### A3.2.5 Input parameters

The fundamental input parameters for the transport solution is the pipe network representation of the discrete fracture network. Each of these pipes has fundamental properties as follows:



- geometric properties: length, width, advective velocity,
- hydraulic properties : transmissivity, storativity
- transport properties: advective velocity, transport aperture, sorption coefficients (by tracer), immobile zone parameter (by tracer and zone, i.e, infilling, altered zone, surrounding rock).

### **A3.2.6 Calibrated parameters**

JNC/Golder expects that most modelling will be carried out as forward modelling, using free water diffusion values, and laboratory values for sorption coefficients, porosities, and diffusion distances. Transport pathways will be analysed with respect to path lengths, widths, and velocity distributions, and the assumptions used in generating the pipe networks (such as the role of fracture intersection zones FIZ) will be adjusted.

### **A3.2.7 Predicted entities and parameters**

JNC/Golder will predict advective travel time for each pathway  $t_{50}$ , percentage mass recovery, and the shape of the breakthrough curve.

### **A3.2.8 Analytical/numerical solution**

Solute transport is solved by the Laplace Transform Galerkin method (LTG) as developed by E. Sudicky (1990). The numerical solution of the primary governing Equation A3-3 is obtained using a standard Galerkin finite element procedure with linear interpolation functions used for each one-dimensional pipe finite element, and a consistent mass matrix formulation applied to the accumulation terms arising from the Laplace transform of the temporal derivative and decay terms.

Details concerning the application of the Galerkin finite element method in the context of the LTG algorithm can be found in e.g. Sudicky (1989), Sudicky (1990), Sudicky and McLaren (1992). Inversion of the nodal Laplace-transformed concentrations is achieved using the discrete Fourier series methodology provided by de Hoog et al. (1982) which employs an efficient quotient-difference algorithm to enhance convergence of the inversion process, thus yielding a high degree of accuracy with relatively few discrete  $p = p_n$  Laplace p-space vectors.

Details concerning the implementation and performance of the de Hoog et al. scheme when applied to the inversion of nodal Laplace-transformed concentrations that arise from an application of the LTG method to solve for transport in fractured geologic media can be found in Sudicky and McLaren (1992).



### **A3.3 References**

**de Hoog, F.R., J. Knight, and A. Stokes, 1982.** An improved method for numerical inversion of Laplace transforms, *SIAM J. Sci. Stat. Comput.*, 3(3), 357-366.

**Sudicky, E.A., 1990.** The Laplace transform Galerkin technique for efficient time-continuous solution of solute transport in double-porosity media, *Geoderma*, 46, 209-232.

**Sudicky, E.A., 1989.** The Laplace transform Galerkin technique: A time-continuous finite element theory and application to mass transport in groundwater. *Water Resour. Res.*, 25(8), 1833-1846.

**Sudicky, E.A. and R. McLaren, 1992.** The Laplace transform Galerkin technique for large-scale simulation of mass transport in discretely fractured porous formations, *Water Resour. Res.*, 28(2), 499-514.



## **SKB/KTH-WRE LaSAR approach summary**



## A4.1 Flow modeling in LaSAR approach

SKB-KTH/WRE will perform a steady state flow modelling of a number of fractures connected serially (head-to-tail). Each fracture is considered as a two dimensional planar fracture with spatially variable aperture. Different fractures have different aperture statistics. There may be leakage of mass at the intersection of the fractures. This leakage is treated as a source/sink term. The flow field is solved using a standard, commercially available code (MODFLOW, 1994).

### A4.1.1 Basic assumptions

The flow is assumed to be steady state. The flow will be determined by solving the following equations with applicable boundary conditions (e.g., constant head).

$$\frac{\partial}{\partial x} \left( T \frac{\partial h}{\partial x} \right) + \frac{\partial}{\partial y} \left( T \frac{\partial h}{\partial y} \right) = s \quad (\text{A4-1})$$

and

$$V = -\frac{\rho g}{3\mu} b^2 \nabla h \quad (\text{A4-2})$$

where the transmissivity  $T$  ( $L^2/T$ ) is related to the half-aperture  $b$  ( $L$ ) as  $T = \frac{2\rho g}{3\mu} b^3$ ,  $s$  is the source/sink term ( $L/T$ ),  $g$  is the gravity acceleration ( $L/T^2$ ),  $\rho$  is the density ( $M/L^3$ ),  $\mu$  is the dynamic viscosity ( $ML^{-1}T^{-1}$ )

### A4.1.2 Geometric concepts

A number of fractures are connected as shown in Figure A4-1. Each fracture is treated as a 2D planar fracture with its own aperture statistics.

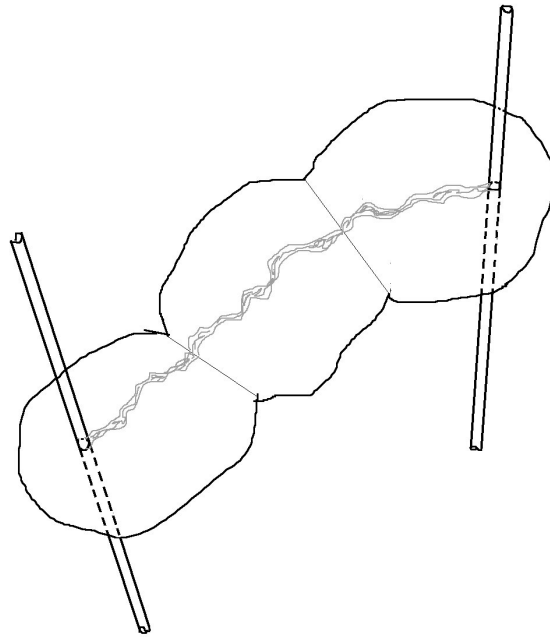


**Figure A4-1** Schematic of connected fractures making up the studied flow path.

Monte Carlo simulations

Objective: Determine  $\tau$ - $\beta$  relationship

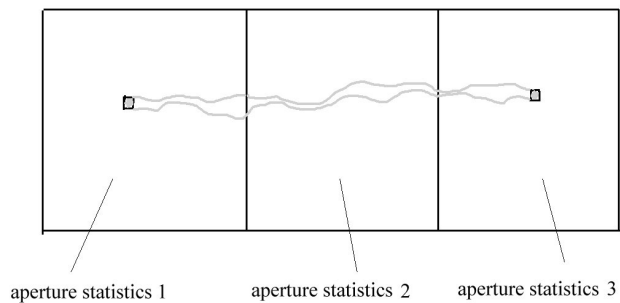


**Figure A4-2** Schematic representation of set up for determination of  $\tau$ - $\beta$  relationship from Monte Carlo simulations.



### **A4.1.3 Input parameters**

To solve the flow field the following input parameters are required:

- $N_{MC}$ , the number of realizations of Monte-Carlo simulations,
- $n_x, n_y$ , the number of the discretized blocks along the x and the y directions, in each realization,
- $dx, dy$ , the size of each element,
- $b(x,y)$ , the aperture of each element, generated randomly in each realization and among different realizations.

### **A4.1.4 Spatial model**

A number of fractures are connected serially in space (Figure A4-2). In the model, each fracture is represented by a domain of rectangular base with variable thickness (aperture).

### **A4.1.5 Model scale**

The modelled scale is about  $50\text{m} \times 20\text{m}$ .

### **A4.1.6 Discretization**

The flow domain is discretized into  $n_x \times n_y$  elements. Each element has the dimension  $dx \times dy \times 2b$ , where  $b$  is the half-thickness (half-aperture) of the element. The aperture varies between different elements.

### **A4.1.7 Numerical solution**

The equation (A4-1) is solved using a standard, commercially available code (MODFLOW, 1994) with finite difference technique to obtain the head in each element. The velocity at the edge between two elements are obtained from (A4-2) using the finite difference method.

## A4.2 LaSAR Transport models

In the flow field, the solute will be transported advectively with the bulk water and be dispersed due to the velocity variation. The solute is also subject to various mass transfer processes. The mass transfer processes include diffusion into rock matrix, sorption in the matrix, diffusion into zones of stagnant water, sorption on fracture surfaces, sorption onto gouge material. The transport problem is solved in two steps. In the first step, a conservative particle is transported only advectively along with the bulk water. The advective transport of the conservative particle is modelled using a particle tracking technique. The residence time in each element is determined when the entrance and the exit points of the particle in the element is established (Mose et al, 1994). This is accomplished in Monte Carlo simulations.

An approximate joint  $\tau$  and  $\beta$  distribution could be determined in the first step; alternatively, we may obtain an approximate  $\beta$ - $\tau$  relationship. In the second step, the particle is dispersed due to velocity variation and is subject to various mass transfer processes. An analytical solution for a pulse input (injection) can be obtained for each mass transfer process along a single flow path. These mass transfer processes are linear. The effect of the coupled processes is obtained by taking the convolution of the individual processes. For a continuous input, the solutions are obtained by the convolution of the continuous input function and the solution for the corresponding pulse input. The effect of dispersion is accounted for by integration over different flow paths characterized by a distribution of  $\tau$  and  $\beta$ .

### A4.2.1 Basic assumptions

The following assumptions are made:

- 1) The tracer is transported only advectively in the fracture;
- 2) All mass transfer processes are linear;
- 3) The advective transport in the rock matrix is negligible. The tracer only diffuses into the rock matrix in the direction orthogonal to the fracture plane;
- 4) Diffusion into the rock matrix is one dimensional;
- 5) The sorption on the inner surfaces of the rock matrix is assumed to be at equilibrium;
- 6) The tracers are fully mixed in the fracture, in the direction orthogonal to the fracture plane;
- 7) The sorption on the fracture surfaces is also assumed to be at equilibrium;
- 8) The sorption onto gouge material is assumed to be first-order kinetically reversible;
- 9) The matrix porosity  $\theta$  and the diffusivity  $D$  in the rock matrix are assumed to be spatially uniform, and identical for all fractures.

### A4.2.2 Conceptual model

The mass balance equations for a solute that is transported into an advection flow path in a single fracture are (Cvetkovic and Dagan 1994)

$$\frac{\partial C}{\partial t} + \frac{\partial C}{\partial \tau} = \sum_i \psi_1^{(i)} \quad (\text{A4-3})$$

$$\frac{\partial N^{(i)}}{\partial t} = \psi_2^{(i)} \quad (\text{A4-4})$$

where  $\tau$  is defined as  $d\tau = dx/V_x$  with  $V_x$  being the flow velocity in the x direction ( $\tau$  is defined in an integral form subsequently). In other words,  $\tau$  is the water residence time along the flow path. The superscript  $i=M,G,S$  referring to the matrix, the gouge material and the stagnant water, respectively. The other variables in Equations A4-3 and A4-4 are:

$C$  = tracer concentration in the fracture [ $\text{ML}^{-3}$ ];

$N^{(i)}$  ( $i=M,G,S$ ) = tracer concentration in the matrix, in the gouge material and in the stagnant water, respectively [ $\text{ML}^{-3}$ ];

$\psi_1^{(i)}$  ( $i=M,G,S$ ) = source/sink terms for the concentration in the fracture related to the matrix, to the gouge material and to the stagnant water, respectively [ $\text{ML}^{-3}\text{T}^{-1}$ ];

$\psi_2^{(i)}$  ( $i=M,G,S$ ) = source/sink terms for the concentrations in the matrix, the gouge material and the stagnant water [ $\text{ML}^{-3}\text{T}^{-1}$ ];

Equations A4-3 and A4-4 may be solved for each individual mass transfer process.

For diffusion into the rock matrix and sorption on the fracture surface, the sink/source term for  $C$  is defined as (Selroos and Cvetkovic 1996; Cvetkovic et al., 1999):

$$\psi_1^{(M)} \equiv \frac{D\theta}{b(\tau)} \frac{\partial N^{(M)}}{\partial z} - \frac{K_a}{b(\tau)} \frac{\partial C}{\partial t} - \lambda C \quad (\text{A4-5})$$

where  $z$  is the coordinate orthogonal to the fracture plane,  $K_a = K_d^f b(\tau)$  is the partition/distribution coefficient for sorption on the fracture surface,  $\theta$  is the matrix porosity and  $D$  is the diffusivity in the rock matrix,  $b(\tau)$  is the Lagrangian half-aperture, obtained through  $b(\tau) \equiv b[\mathbf{X}(\tau)]$ , where  $\mathbf{X}(t)$  is the advection trajectory and  $\lambda$  is the spontaneous decay constant if the solute is radioactive. For a non-radioactive solute, there is no decay term.

The source/sink term in the matrix is defined as

$$\psi_2^{(M)} \equiv -K_d^m \frac{\partial N^{(M)}}{\partial t} - \lambda N^{(M)} + D \frac{\partial^2 N^{(M)}}{\partial z^2} \quad (\text{A4-6})$$

where we assume equilibrium sorption in the matrix with  $K_d^m$  being the distribution coefficient.

### A4.2.3 Immobile zone

For sorption onto gouge material, we assume the sorption to be first-order kinetically reversible, formulated as the two-site model (Cvetkovic et al, in press):

$$\psi_1^{(G)} \equiv -K_d^g \alpha C + \alpha N^{(G)} - \lambda C \quad (\text{A4-7})$$

$$\psi_2^{(G)} \equiv -K_d^g \alpha C + \alpha N^{(G)} - \lambda N^{(G)} \quad (\text{A4-8})$$

where  $K_d^g$  is the distribution coefficient for the sorption onto gouge material, and  $\alpha$  is the mass transfer rate. For simplicity, we assume that  $K_d^g$  and  $\alpha$  are constant, i.e., independent of  $\mathbf{x}$  (or  $\tau$ ).

### A4.2.4 Integration of flow and transport

Both the flow and the transport are modelled in a few serially connected fractures. The particle tracking is performed in the velocity field provided by the flow model.

### A4.2.5 Input parameters

- geometrical properties:  $n_x, n_y, dx, dy$ ;
- number of particles and the initial positions of the particles;
- information for the source/sink terms ( position, intensity);
- advective velocity field;
- diffusion and sorption parameters;
- input (injection) function.

#### A4.2.6 Calibrated parameters

- multiplying factor for transmissivity (or aperture) if necessary;
- multiplying factor for B;
- parameters for sorption onto gouge material  $K_d^g$  and  $\alpha$

#### A4.2.7 Predicted entities and parameters

- breakthrough curve for each tracer and each test including  $t_5$ ,  $t_{50}$ ,  $t_{95}$ ;
- mass recovery;

#### A4.2.8 Analytical and numerical solution

The advective transport of the conservative particle is modelled using a particle tracking technique. The residence time in each element is determined when the entrance and the exit points of the particle in the element is established (Mose et al, 1994).

For a *single fracture*, the solution of Equations A4-3 and A4-4 with the source terms of matrix diffusion/sorption, cf. Equations A4-5 and A4-6, for a pulse input (injection) with zero initial conditions is;

$$\gamma^{(M)}(t, \tau; \beta) = \frac{H(t - \tau)}{2\sqrt{\pi}(t - \tau - B_a)^{3/2}} \exp\left[\frac{-B^2}{4(t - \tau - B_a)} - \lambda t\right] \quad (\text{A4-9})$$

where

$$B(L) = \int_0^L \frac{\theta(x)\sqrt{D(x)R_m(x)}dx}{V_x(x)b(x)} \quad B_a(L) = \int_0^L \frac{K_a(x)dx}{V_x(x)b(x)}$$

and  $R_m = 1 + K_d^m$ ,  $L$  is the distance between the injection and extraction boreholes.  $V_x(x)$  and  $b(x)$  are *Lagrangian* quantities that follow a flow path, e.g.  $V_x(x) \equiv V_x\{X[\tau(x)]\}$ . Also, we have

$$\tau(L) = \int_0^L \frac{dx}{V_x(x)}$$

where  $\tau(L)$  is the water residence time between the injection point  $x=0$  and the extraction point  $x=L$ .

For  $N$  *serially connected fractures* where  $\kappa$  and  $K_a$  are uniform, we have

$$B = \kappa \beta = \kappa \sum_{i=1}^N \beta_i \qquad B_a = K_a \beta = K_a \sum_{i=1}^N \beta_i$$

where

$$\beta_i(L_i) = \int_0^{L_i} \frac{dx}{V_x(x)b(x)}$$

The solution of Equations A4-3 and A4-4 with the source terms of the sorption onto gouge material, cf. Equations A4-7 and A4-8, for a pulse input with zero initial conditions is:

$$\gamma^{(G)}(t, \tau) = e^{-\alpha K_d^g \tau} \delta(t - \tau) + \alpha^2 K_d^g \tau \exp\{-\alpha[K_d^g \tau + (t - \tau)]\} \tilde{I}_1[\alpha^2 K_d^g (t - \tau)]$$

where  $\tilde{I}_1(Z) \equiv I_1(2Z^{1/2})/Z^{1/2}$  with  $I_1$  being the modified Bessel function of the first kind of order one.

The solution for the coupled mass transfer processes is obtained by taking the convolution (with respect to t) of the solutions of each individual process:

$$\gamma(t, \tau) = \gamma^{(M)} * \gamma^{(G)}$$

where "\*" is the convolution operator.

For a continuous input  $\phi(t)$ , and including spreading along different flow paths, the solution is

$$Q(x, t) = \int_0^\infty \int_0^\infty [\phi(t) * \gamma(t, \tau; \beta)] g(\tau, \beta; x) d\tau d\beta$$

where  $g(\tau, \beta; x)$  is the joint distribution of  $\beta$  and  $\tau$ .

### **A4.3 References**

**Cvetkovic, V., and Dagan, G. 1994 :** Transport of kinetically sorbing solute by steady random velocity in heterogeneous porous formations, *J. Fluid Mech.*, v. 265, pp. 189-215.

**Cvetkovic, V., Selroos, J.-O., and Cheng, H. 1999 :** Transport of reactive tracers in rock fractures, *J. Fluid Mech.*, v. 378, pp. 335-356.

**Cvetkovic, V., H. Cheng and J.O. Selroos (in press) :** Evaluation of TRUE-1 sorbing tracer experiments at Äspö: Theory and applications, SKB International Cooperation Report.

**MODFLOW/EM 1994 :** The USGS Three Dimensional Ground Water Flow Model, Maximal Engineering Software, Inc, 1994.

**Mose, R., Siegel P., and Ackerer P. 1994 :** Application of the mixed hybrid finite element approximation in a ground water flow model: Luxury or necessity? *Water Resour. Res.*, 30, 3001-3012, 1994

**Selroos, J. O., and Cvetkovic, V. 1996 :** On the characterization of retention mechanisms in rock fractures, SKB Technical Report TR 96-20.





## **POSIVA/VTT Approach summary**



## A5.1 POSIVA Transport model

Transport is assumed to take place along a single channel. The velocity field in the channel is assumed to be linear. The mean concentration across the channel can be solved analytically (Hautojärvi and Taivassalo 1994) if only the advective field and molecular diffusion is taken into account. The mean concentration can be expressed by

$$C_m = \frac{1}{2} \left( \operatorname{erf} \left[ \frac{\frac{1}{2} X_s + X + \xi_1}{2\sqrt{\xi_2}} \right] + \operatorname{erf} \left[ \frac{\frac{1}{2} X_s - X - \xi_1}{2\sqrt{\xi_2}} \right] \right);$$

$$\xi_1 = -\frac{1}{2} \tau; \quad \xi_2 = \left( \frac{1}{(Pe)^2} + \frac{1}{120} \right) \tau - 8 \sum_{n=0}^{\infty} \frac{1 - e^{-(2n+1)^2 \pi^2 \tau}}{(2n+1)^8 \pi^8}; \quad (\text{A5-1})$$

$$\tau = \frac{Dt}{a^2}; \quad X = \frac{Dx}{a^2 u_0}; \quad X_s = \frac{Dx_s}{a^2 u_0}; \quad Pe = \frac{a u_0}{D}$$

where

$D$  is the molecular diffusion coefficient,  
 $a$  is the width of the velocity profile,  
 $x_s$  is the initial width of the tracer plume,  
 $u_0$  is the maximum flow velocity,  
 $t$  is the time and  
 $x$  is the position along the channel.

The maximum flow velocity,  $u_0$ , is calibrated to the measured total flow rate through the channel. For this calibration also the volume aperture of the fracture should be known. The latter is estimated using the transmissivities of the borehole sections and applying the calibrated ratio of the volume and hydraulic apertures, if there exists suitable tracer tests data for the calibration, or by using calibrated value from the TRUE-1 experiments, in the case suitable tracer tests data does not exist. Surface sorption can be taken into account at the maximum velocity.

The output of the Equation A5-1 describes the breakthrough in the case that matrix diffusion is not taken into account. Matrix diffusion can be now be included by convoluting the output of Equation A5-1 with matrix diffusion response using the following relationship.

$$f(t) = \int_0^t g(z) \frac{\operatorname{Exp} \left( -\frac{u^2}{t-z} \right)}{\sqrt{\pi} (t-z)^3} dz \quad (\text{A5-2})$$

where  $g(z)$  is the output of Equation (A5-1) and

$$u = \sqrt{D_e K_d \rho_s} \frac{W L}{Q} \quad (\text{A5-3})$$

where  $D_e$  is the effective diffusion coefficient of the rock matrix,  $K_d$  is the distribution coefficient,  $\rho_s$  is the density of the rock matrix,  $W$  is the width and  $L$  the length of the flow channel and  $Q$  is the flow rate in the flow channel.

## A5.2 POSIVA supporting DFN flow modelling

Supporting DFN flow modelling is based on the simulations using heterogeneous fractures and solving of the flow field with the FEFTRA code (Reference) according to the equation (Bear 1979)

$$S \frac{\partial h}{\partial t} - T \frac{\partial^2 h}{\partial x^2} = q \quad (\text{A5-4})$$

where  $h$  is hydraulic head,  $S$  is storativity,  $T$  is transmissivity and  $q$  is source or sink. Using the solved head field the streamlines are followed using calculated flow velocity at the node points

$$v(x, y) = \sqrt[3]{\frac{\rho g}{12\mu}} T(x, y)^{2/3} \nabla h(x, y) \quad , \quad (\text{A5-5})$$

Based on the streamlines the length of the flow path is calculated. The variation of the width of the flow channel can also be studied by following the streamlines starting from the injection borehole.

## A5.3 References

**Bear, J., 1979.** Hydraulics of groundwater, McGraw-Hill Inc, 1979.

**Hautojärvi, A. and Taivassalo, V., 1994.** The Intraval Project -Analysis of the Tracer Experiments at Finnsjön by the VTT/TVO Project Team. Nuclear Waste Commission of Finnish Power Companies. Report YJT-94-24.